UNIVERSITÀ
DEGLI STUDI
DI BRESCIA

DOTTORATO DI RICERCA IN PRECISION MEDICINE

settore scientifico disciplinare BIO/14 FARMACOLOGIA

CICLO
XXXVI

AdrenoCortical Carcinoma: in search of new pharmacological strategies

PhD Student: Andrea Abate

SUPERVISOR: Prof. Sandra Sigala

Abstract (English)

Adrenocortical carcinoma (ACC) is a rare malignancy with a dismal prognosis. The pharmacological approach of ACC is based on mitotane (M) with/without etoposide (E), doxorubicin (D) and cisplatin (C) (the EDP-M scheme), according to the disease stage. Considering the limited efficacy and the toxicity of this treatment, new strategies are required. ACC is a heterogeneous tumour, thus, the paucity of ACC cell models arising from EDP-M-resistant metastatic/advanced disease has also been a limitation in the preclinical evaluation of new pharmacological strategies for decades. Here we report the development of a new ACC cell line, named TVBF-7, derived from a patient with metastatic disease progressing after EDP-M. TVBF-7 cells have been shown to secrete high amounts of cortisol and they harbors a nonsense mutation in APC gene. Using the preclinical experimental ACC cell models, namely TVBF-7 cells and other cell lines,we studied the effect on ACC of evaluated two drugs currently used in the pharmacological management of other tumours: ribociclib and trabectedin.

Ribociclib is a member of the target-therapy family of drugs inhibiting CDK4/6. Evidence indicates cell cycle-targeted drugs, such as CDK4/6-inhibitors, as a potentially relevant therapeutic strategy in ACC. We evaluated the effect of ribociclib in cell models of ACC, both as a single treatment and in a combination context with mitotane and/or progesterone. The combination of ribociclib with hormone therapy is a strategy already used in other malignancies, such as in some types of breast cancer. Interestingly, our research group demonstrated at preclinical level a role of progesterone as ACC anticancer drug. Here we reported a cytotoxic and antiproliferative activity of ribociclib in ACC cell models. The effect on cell viability was enhanced when ribociclib was combined with progesterone and/or mitotane. The positive relationship underlined by our results between ribociclib, progesterone and mitotane strengthen the clinical potential of this combination.

Trabectedin is a DNA-binding agent, with a complex mechanism of action, which also involves interaction with the tumour microenvironment. The DNA alkylation appears to be a critical point for the cytotoxic and antiproliferative effect in ACC. We have previously demonstrated the long-lasting cytotoxic effect of trabectedin in several cell models of ACC. Furthermore, we reported an inhibitory effect on Wnt signalling pathway, a driver pathway of ACC, in the human ACC cell line NCI-H295R. Here we evaluated the effect of trabectedin on invasion/metastasis processes in different preclinical models of ACC. Xenograft experiments demonstrated that trabectedin significantly reduced the tumour area in each ACC cell model and metastasis formation in embryos injected with metastasis-derived cell lines. Trabectedin treatment reduced the invasiveness of ACC cells across the matrix, which was greater at baseline for the metastatic models. In metastatic cell models, protein analysis demonstrated a reduction of MMP2 secretion and activity in the culture medium after treatment. In conclusion, our results indicate that trabectedin interferes with invasiveness and metastasis processes, both dramatic feature of ACC.

Abstract (Italiano)

Il carcinoma della corticale del surrene (ACC) è un tumore raro con una cattiva prognosi. L'approccio farmacologico all'ACC è basato sul mitotano (M) con/senza etoposide (E), doxorubicina (D) e cisplatino (C) (schema EDP-M), in base allo stadio della malattia. Considerata la limitata efficacia e la tossicità di questo trattamento, è richiesta l'individuazione di nuove strategie. Considerata l'eterogeneità dell'ACC, la mancanza di modelli cellulari derivanti da malattia metastatica/avanzata resistente ad EDP-M ha rappresentato un limite per decenni negli studi preclinici. Qui riportiamo lo sviluppo di una nuova linea cellulare di ACC, chiamata TVBF-7, derivante da un paziente con malattia metastatica in progressione dopo EDP-M. Le cellule TVBF-7 secernono quantità elevate di cortisolo e presentano una mutazione non senso nel gene APC. Utilizzando il modello sperimentale preclinico rappresentato dalle cellule TVBF-7 e altre linee cellulari, abbiamo studiato l'effetto di due farmaci in ACC attualmente utilizzati nel management farmacologico di altri tumori: ribociclib e trabectedina.

Ribociclib è un membro della famiglia di farmaci della target-therapy che inibiscono CDK4/6. Vi sono evidenze che i farmaci che hanno come target il ciclo cellulare, quali gli inibitori di CDK4/6, rappresentino una strategia terapeutica potenzialmente rilevante nell'ACC. Abbiamo valutato l'effetto di ribociclib in modelli cellulari di ACC, sia come trattamento singolo che in combinazione con mitotano e/o progesterone. La combinazione di ribociclib con la terapia ormonale è una strategia già utilizzata in altre neoplasie, come in alcuni tipi di tumore al seno. È interessante notare che il nostro gruppo di ricerca ha dimostrato a livello preclinico un ruolo del progesterone come farmaco antitumorale per l'ACC. I risultati qui riportati indicano un'attività citotossica e antiproliferativa di ribociclib in modelli cellulari di ACC. L'effetto sulla vitalità cellulare è stato potenziato quando ribociclib è stato combinato con progesterone e/o mitotano. La relazione positiva tra ribociclib,

mitotano e progesterone sottolineata dai nostri risultati rafforza il potenziale clinico di questa combinazione.

La trabectedina è un agente legante il DNA, con un meccanismo d'azione complesso, che prevede anche l'interazione con il microambiente tumorale. L'alchilazione del DNA sembra essere un meccanismo critico per l'effetto citotossico e antiproliferativo in ACC. Precedentemente abbiamo dimostrato l'effetto citotossico a lunga durata della trabectedina in diversi modelli cellulari di ACC. Inoltre, abbiamo dimostrato un effetto inibitorio sul pathway di Wnt, un driver-pathway dell'ACC, nella linea cellulare di ACC umano NCI-H295R. Qui abbiamo valutato l'effetto della trabectedina sui processi di invasione/metastasi in diversi modelli preclinici di ACC. Gli esperimenti di xenotrapianto hanno dimostrato che la trabectedina riduce significativamente l'area tumorale per ciascun modello cellulare di ACC e la formazione di metastasi negli embrioni iniettati con linee cellulari derivate da metastasi. Il trattamento con trabectedina ha ridotto l'invasività delle cellule di ACC attraverso la matrice, la quale era maggiore al basale per i modelli metastatici. Nei modelli cellulari metastatici abbiamo dimostrato una riduzione della secrezione e dell'attività di MMP2 nel terreno di coltura dopo il trattamento. In conclusione, i nostri risultati indicano che la trabectedina interferisce con l'invasività ed i processi di metastasi, entrambi aspetti drammatici dell'ACC.

Summary

1 Introduction

1.1 The adrenal glands

1.1.1 Structure and development

The adrenal glands are two retroperitoneal endocrine organs located at the apical pole of each kidney. Macroscopically, they are characterized by a triangular shape with a volume of approximately 3 – 6 cm^3, weighing about 6 – 11 grams [1, 2]. Each gland consists of two functionally region: the outer cortex and the inner medulla. The cortex is surrounded on the outside by a thick capsule consisting of connective tissue and has three distinct functional and histological zones:

- the zona glomerulosa is located under the capsule and is composed of small polyhedral cells arranged in groups wound like rosettes.
- the zona fasciculata is the largest and is located in an intermediate position; it is composed of polyhedral cells arranged in radial cords.
- the zona reticularis is the deepest portion of the adrenal cortex and is composed of an irregular network of cords of rounded cells.

The medulla is located at the center of the gland, surrounded by the cortex except for the area corresponding to the hilum. This region is composed by irregularly shaped cells (chromaffin cells) grouped around blood vessels that are modified postganglionic neurons and preganglionic autonomic nerve fibers lead to them directly from the central nervous system [3-5] (Figure 1.1).

Embryologically, the cortex derives from the mesoderm, while the medulla derives from the neural crest. The development of the adrenal glands is mediated by steroidogenic factor 1 (SF1), Cbp/p300-interacting transactivator 2 (CITED-2), β-catenin, and other factors. The adrenal gland first appears 28-30 days post-conception [6-8].

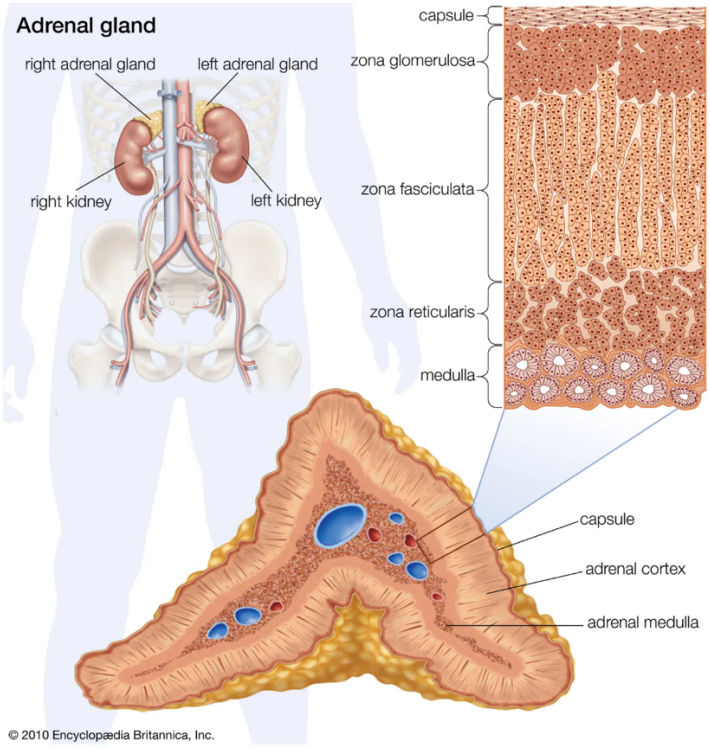

Figure 1.1 Anatomy and structure of the human adrenal gland

(Encyclopedia Britannica, 2010)

1.1.2 Physiology

The adrenal gland represents a complex endocrine tissue involved in the maintenance of the body homeostasis. From a functional point of view, the cortex produces steroid hormones, and the medulla produces the catecholamines [2, 9]. Adrenal cortex function is mostly regulated by the adrenocorticotropic hormone (ACTH), produced in the pituitary gland [10], while the adrenal medulla is responsive to the sympathetic nervous system [11].

Each area of the cortex produces steroid hormones from the precursor cholesterol (Figure 1.2). In the adrenal cell, the regulation of cholesterol transport from the outer mitochondrial membrane to the inner mitochondrial membrane is ensured by the steroidogenic acute regulatory protein (StAR). In the inner mitochondrial membrane, the cholesterol is converted to pregnenolone by the CYP11A1 enzyme [12]. This enzyme catalyzes the rate-limiting step of steroid hormone production, and it is expressed in all three layers of the adrenal cortex. ACTH induces steroidogenesis in all three zones

by stimulating CYP11A1 [10]. The downstream fate of pregnenolone will depend on the specific enzymes within that zone:

- *In the zona glomerulosa*, 17-alpha-hydroxylase is not expressed and pregnenolone can only be converted to progesterone via 3-beta-dehydrogenase; 21-hydroxylase catalyzes conversion to 11-deoxycorticosterone; 11-beta-hydroxylase catalyzes conversion to corticosterone. Finally, aldosterone synthase, which is present only in the zona glomerulosa and is regulated by angiotensin II, converts corticosterone into aldosterone. Aldosterone, corticosterone, and deoxycorticosterone have mineralocorticoid activity, with aldosterone being the predominant mineralocorticoid in humans [13].

- *In the zona fasciculata*, 17-alpha-hydroxylase converts pregnenolone and progesterone, which were synthesized in the glomerulosa, into 17-hydroxypregnenolone and 17-hydroxyprogesterone, respectively; 3-beta-dehydrogenase converts 17-hydroxypregnenolone into 17-hydroxyprogesterone; 21-hydroxylase converts 17-hydroxyprogesterone to 11-deoxycortisol; and 11-beta-hydroxylase converts 11-deoxycortisol to cortisol, the predominant glucocorticoid [13].

- *In the zona reticularis*, 17-hydroxypregnenolone and 17-hydroxyprogesterone can be converted into DHEA and androstenedione by 17,20 lyase (17 alpha-hydroxylase). Although DHEA is predominantly made, some of it can be converted into androstenedione by 3ß-hydroxysteroid dehydrogenase in the zona reticularis [13].

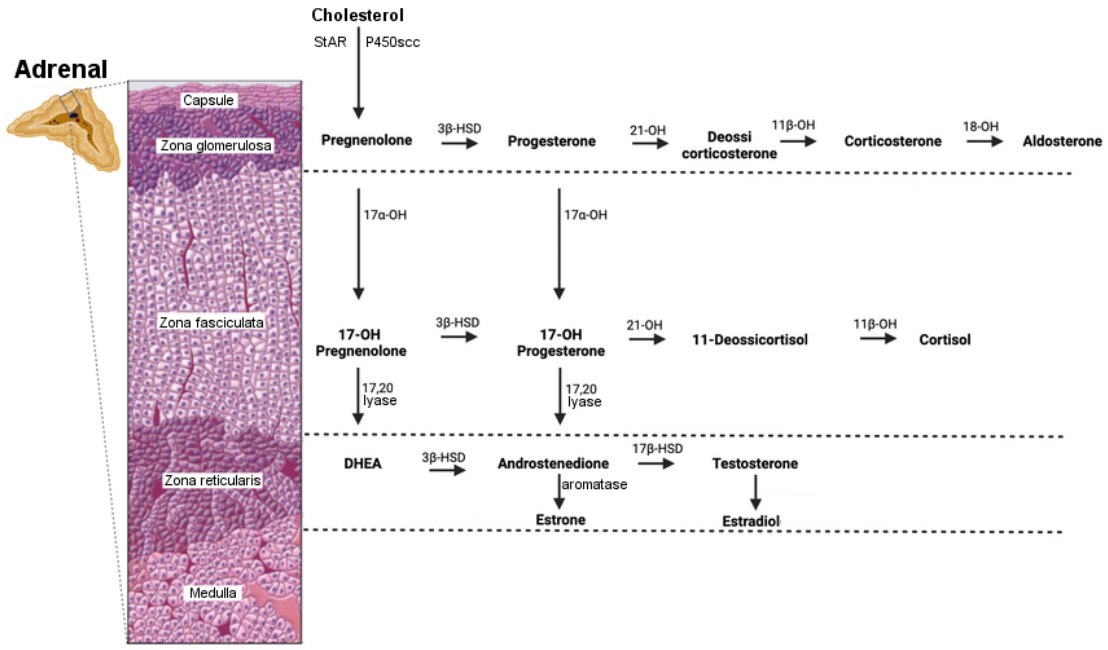

Figure 1.2 Schematic of the classical adrenal steroidogenesis biosynthesis pathway. Modified from [14]

During stress, the adrenal hormones induce various protective changes, which ultimately contribute to the restoration of body homeostasis. Both glucocorticoids and catecholamines are known to acutely increase plasma glucose levels, promote elevated cardiac output, maintain high blood pressure, and to suppress inflammation [9].

1.1.3 Pathology: the adrenal tumors

There are many conditions that can alter the functionality of the adrenal gland, including tumors [15]. Adrenal tumors can affect both the cortex (adrenocortical tumors) and the medulla (pheochromocytomas). Adrenocortical tumors include benign and malignant neoplasms, named adrenocortical adenomas (ACA) and carcinomas (ACC), respectively. Similarly, pheochromocytomas can be either of benign or malignant origin [16].

1.2 Adrenocortical carcinoma

1.2.1 Epidemiology

The adrenocortical carcinoma (ACC) is a rare aggressive malignancy, with a poor prognosis. The annual incidence of ACC is 0.7 – 2.0 patients per million people per year. ACC can occur at any age, with a first peak in the pediatric population (<5 years of age) and a second peak during the fourth to fifth decades of adult life [17-19]. Interestingly, the incidence of pediatric ACC is 10 –15 times higher in children in southern Brazil, which is related to an inherited germline p53 mutation [20, 21]. A slight gender difference is observed, with the women more affected (55–60%) than men [17].

1.2.2 Pathogenesis and genetics

The pathogenesis of ACC is also heterogeneous and not yet fully understood. Although mainly sporadic with no identifiable risk factor, ACC may be a part of hereditary syndromes [17, 22], such as:

- Lynch syndrome characterized by mutations on genes involved in DNA mismatch repair genes, namely MLH1, MHS2, MHS6, EPCAM and PMS2 [23].
- Li-Fraumeni syndrome (LFS) which is often associated with a pathogenic or likely pathogenic mutation in the TP53 gene [24].
- The multiple endocrine neoplasm type 1, with a mutation on MEN1 gene [25].
- Familial adenomatous polyposis (FAP), characterized by an inactivating germline mutation of the tumor suppressor gene Adenomatous Polyposis Coli (APC) gene, which encodes for a downstream regulator of the Wnt/β-catenin pathway [26].
- Beckwith–Wiedeman syndrome (BWS) with an alterations of DNA methylation of the 11p15 locus, which harbors the coding regions for Insulin-Growth-Factor 2(IGF2), the cell cycle regulator CDKN1C, and the non-translated RNA, H19 [27].

In sporadic ACC, the most frequently reported somatic mutations are affecting p53 signaling, Wnt/β-catenin signaling, and IGF2 overexpression [28-30]. Signaling of the Wnt family is one of the pivotal mechanism directing cell proliferation and cell fate determination during embryonic development and in adult organs, with β-catenin being the key effector responsible for transduction of the signal to the nucleus [31]. Within this pathway, the most common genetic abnormalities identified in ACC are the activating mutations of the Catenin Beta 1 gene (CTNNB1), and the deletions in the Zinc and Ring Finger 3 (ZNFR3) gene, that lead to activation of the Wnt/β-catenin pathway in ACC [28-30]. Consequently, activation of the Wnt pathway induces cell proliferation and resistance to apoptosis. Furthermore, the somatic mutation of the CTNNB1 is an independent predictor of poor survival in ACC [32]. The TP53 gene encodes a multi-domain homo-tetrameric transcription factor with a large amount of direct transcriptional target genes. The p53 protein plays a central role in the cell's response to genotoxic stress by activating pathways involved in cell cycle arrest and DNA damage repair. The p53-mediated responses could allow cells to respond to stress and to repair accumulated DNA damage. However, if the damage to the genome is irreparably compromised, p53 induces apoptosis to avoid the propagation of a corrupted genome. In addition to these roles, p53 is known to mediate cellular angiogenesis and senescence and it has recently been recognized to participate in the inflammatory response and suppression of invasiveness. Based on these multiple roles, impaired p53 activity can result in malignancies [33]. The IGF pathway is involved in the development and in the maintenance of different biological functions in normal adrenal glands [34]. Interestingly, the IGF2 gene is highly overexpressed in majority of ACCs [35], it regulates the growth and apoptosis of cells and interact with IGF1 receptor (IGF1R), that is as well frequently overexpressed in ACC [36]. Activation of IGF1R results in the stimulation of downstream signaling pathways including the mitogen-activated protein kinase (MAPK) and phosphoinositide-3-kinase/AKT (PI3K/AKT) pathway, leading to increased cell proliferation and survival [37]. Of note, IGF2 overexpression by loss of heterozygosity (LOH) is associated with poorer outcome in ACC [38].

1.2.3 Clinical presentation

ACC may present with a clinically significant hormone excess or with symptoms caused by an abdominal mass. An increasing number (approximately 10–15%) of adrenal incidentaloma are diagnosed as ACC [39, 40]. About 50–60% of patients with ACC have clinical hormone excess: hypercortisolism (Cushing syndrome) or mixed Cushing and virilizing syndromes are observed in most of these patients. Pure androgen excess is less frequent, while estrogen or mineralocorticoid excess is very rare [41-44]. Non-specific symptoms from an abdominal mass include abdominal discomfort (nausea, vomiting, abdominal fullness) or back pain. Classical malignancy-associated symptoms such as weight loss, night sweats, fatigue or fever are rarely present [17].

1.2.4 Diagnosis

The ACC working group of the European Network for the Study of Adrenal Tumors (ENS@T) has proposed guidelines for diagnostic procedures. Each patient with suspected and proven ACC should be discussed in a multidisciplinary expert team meeting and should undergo a careful clinical assessment, detailed endocrine work-up to identify autonomous hormone excess and adrenal-focused imaging. Additional imaging (e.g., bone and brain imaging) are recommended only in case of clinical suspicion of metastatic lesions. The adrenal biopsy is not recommended, because of the increased risk of (needle-tract seeding) metastases, unless there is evidence of metastatic disease that precludes surgery and histopathologic proof is required to inform oncological management [17].

1.2.5 General prognosis

The prognosis of ACC is heterogeneous according to tumor stage based on the ENS@T classification [45]. The 5-year survival is 60–80% for tumors confined to the adrenal space, it is reduced to 35–50% in case of locally advanced disease, and it is from 0% to 28% for metastatic disease [17]. Other independent prognostic factors are the resection status [46], the mitotic index Ki67 [47] and cortisol excess [41]. Particularly, incomplete microscopic or macroscopic resection,

high mitotic index (Ki67 >20%) and hypercortisolism are associated with the worst prognosis. A multicenter ENS@T study proposed the use of a score (S-GRAS) based on the combination of clinical and histopathological parameters (including ENS@T stage, grading defined by Ki67 index, resection status, age and symptoms due to steroid autonomous secretion or tumor mass) to improve prognostication in ACC patients [48].

1.2.6 Treatments

To date, the greatest chance of survival for patients with an early-stage disease is provided by radical surgery. The ENS@T guidelines recommend surgery performed only by surgeons experienced in adrenal and oncological surgery [17]. However, in about a half of patients the diagnosis of ACC occurs when the disease is already metastatic and not eligible for surgery. Moreover, 30–70% of radically operated patients recur within two years, often with metastatic disease [17, 49].

Current pharmacotherapy for ACC is based on the adrenolytic drug mitotane, a derivative of dichlorodiphenyltrichloroethane (DDT). Mitotane is an adrenal-specific cytotoxic agent that inhibits sterol-O-acyl transferase (SOAT1) [50], however the mechanism of cytotoxicity in ACC cells is not fully understood. Due to the adrenolytic effect, mitotane induces adrenocortical insufficiency. For this reason, the drug must be administered in association with glucocorticoid replacement therapy [51, 52]. Repeated evidence demonstrated that the drug is fully active when it reaches plasma concentrations above/equal 14 mg/L, while values greater than 20 mg/L are associated with central neurological toxicity. Due to the complex mitotane pharmacokinetic, achieving plasma concentrations within the therapeutic window requires no less than 2–3 months [53-55].

Mitotane is used both in the adjuvant approach in patients at high risk of recurrence and in cases of advanced/metastatic disease that cannot be treated surgically [17]. Mitotane is prescribed as single agent in patients with oligometastatic disease with an indolent course [49], in association with local regional approaches such as radio-frequency ablation (RFA), trans-arterial chemoembolization

(TACE), or radiotherapy [18]. In other cases, the drug is administered in association with the EDP chemotherapy (etoposide, doxorubicin, and cisplatin), the EDP-M approach [17, 56-58]. The efficacy of this therapeutic scheme in advanced ACC was demonstrated in comparison with the streptozotocin-mitotane scheme in a randomized phase III clinical trial, called FIRM-ACT [56].

There are no standard treatment options in patients progressing to EDP-M. The gemcitabine and capecitabine regimen, although occasionally effective, has not shown to improve patient outcome [59-61]. Therefore, few effective therapeutic options are currently available in patients with ACC and new therapeutic strategies are needed.

1.3 Possible pharmacological strategies in ACC

In recent years, the number of preclinical and clinical studies aimed at evaluating new pharmacological strategies in ACC has increased. The need to identify effective pharmacological treatments, especially in the context of advanced ACC, remains a hot topic in scientific research. Efforts are focused on multiple fronts: cytotoxic drugs, radioligands, targeted therapies and immunotherapy agents. In patients with advanced/metastatic disease, modern targeted therapies have shown significant cytotoxicity in preclinical studies; however, studies conducted on patients with ACC have so far reported disappointing results. The absence of targeted agents that specifically inhibit the main molecular pathways of ACC growth is the main cause of the failure of these drugs [62].

1.3.1 Ribociclib

Ribociclib (LEE01, Figure 1.3), palbociclib and abemaciclib are a selective cyclin-dependent kinase (CDK) 4 and 6 inhibitors. These kinases are activated upon binding to D-cyclins and play a crucial role in signalling pathways which lead to cell cycle progression and cellular proliferation. The cyclin D-CDK4/6 complex regulates cell cycle progression through phosphorylation of the retinoblastoma protein (pRb) [63]. Evidence indicates that cell cycle-targeted drugs represent a potentially relevant therapeutic strategy in ACC [64]. Moreover, CDK4 gene was found overexpressed in more than 60% of ACC samples [65].

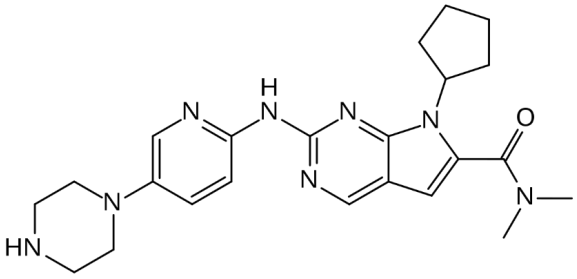

Figure 1.3 Ribociclib (LEE011)

The three CDK4/6 inhibitors are all orally bioavailable, small molecules. Ribociclib and palbociclib appear to have greater lipophilicity and larger binding site side chains compare to abemaciclib, which might reduce the number of off-target kinase ATP-binding pockets they interact with [66]. Interestingly, in chemo-proteomics study of CDK4/6 inhibitor activity in lung carcinoma cell lines and primary tumour samples, ribociclib was found to be significantly more selective towards CDK4 and CDK6 than palbociclib [67].

Ribociclib has demonstrated antitumor activity in preclinical and clinical studies of a wide variety of tumour types, including breast cancer, melanoma, and neuroblastoma. Although it has been shown that ribociclib is active as single agent, the combination with other drugs acting on these cancers enhances the treatment efficacy and it delays the development of treatment resistance in both preclinical and clinical studies [63]

1.3.2 Trabectedin

Trabectedin (ET-743) is a powerful anti-tumor drug initially isolated from the Caribbean tunicate *Ecteinascidia turbinate* (Figure 1.4). In particular, the compound is produced by a symbiont bacterium, *Candidatus Endoecteinascidia frumentensis* [68]. The marine extract was found to possess anticancer activity during a research campaign funded by the National Cancer Institute (NCI, USA) in 1969 [69]. The Food and Drug Administration (FDA) and the European Medicines Agency (EMA) approved trabectedin for treatment of soft tissue sarcoma after failure of anthracyclines and ifosfamide, or who are not amenable to receive these agents. The drug is also approved by EMA for treatment of patients with relapsed platinum-sensitive ovarian cancer in combination with pegylated liposomal doxorubicin [70, 71].

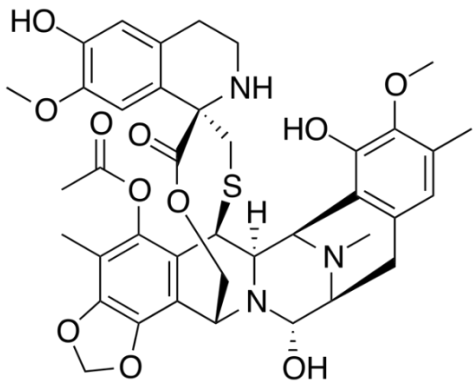

Figure 1.4 Trabectedin (ET-743)

Trabectedin is an alkylating agent, but, unlike other molecules of the class which bind the major groove of DNA, trabectedin interferes with the minor groove, particularly binding guanine on the exocyclic N2 amino group [72]. The molecule directly interferes with the activated transcription, it impairs the transcription-coupled nucleotide excision repair (TC-NER) system, and it induces DNA double-strand breaks [73-79]. All these effects are caused by the covalent bond of trabectedin with DNA, but also to a direct interaction of part of the molecule protruding from the DNA, with specific factors involved in DNA transcription and repair. Multiple mechanisms are involved in the inhibition of active transcription induce by trabectedin, i.e. it has been shown a direct block of RNA polymerase II during transcription and the consequent rapid degradation of the enzyme via the proteasome pathway [79]. Furthermore, the displacement of oncogenic transcription factors from their target promoters and the inhibition of DNA separation during the transcription have been also demonstrated [79, 80]. Interestingly, the active transcription of the MDR1 gene coding for the multidrug resistance pump P-glycoprotein (P-gp) is recognized to be down-regulated by trabectedin [81]. Furthermore, the high expression of P-gp causes resistance to chemotherapeutic agents in several tumors, including ACC [82]. Furthermore, trabectedin was also found to inhibit the Wnt signaling pathway in human biliary tract carcinoma preclinical cell models [83].

Several studies have been conducted on cell lines with well-defined defects of DNA repair mechanisms. Evidence suggested a role for transcription-coupled nucleotide excision repair (TC-

NER) and homologous recombination in the cytotoxic activity of trabectedin, whereas the mechanism of mismatch repair deficiency status does not affect it. Particularly, TC-NER–deficient cells are 2 to 10 times less sensitive to trabectedin. This is a peculiar characteristic for this compound and it contrasts with what has been reported for other DNA-damaging agents used in the treatment of cancer (e.g. cisplatin) [83].

Trabectedin is also able to modify the tumor microenvironment (TME) [84, 85]. It is well known that TME plays a crucial role in the development of the tumor and that modifications at this level can be exploited pharmacologically. It has been observed that this drug is able to rapidly induce apoptosis in tumor-associated macrophages (TAMs), furthermore it determines the reduction of inflammatory mediator synthesis, such as CCL2, CXCL8, IL6, VEGF and PTX3 by monocytes, macrophages and TAMs. The alteration of the production of inflammatory mediators is of fundamental importance to alter those mechanisms that allow the tumor to grow and proliferate [84, 85].

1.4 Adrenocortical preclinical cell models

To date, several ACC cell lines are available. There are six cell lines derived from human ACC that share the consensus regarding their use as models of this pathology (Figure 1.5). Furthermore, several primary cultures of ACC are used in preclinical studies.

The first human ACC cell line NCI-H295, derived from a primary ACC in a female patient was reported in 1990. NCI-H295R cells, the most known and used sub-clone, have been reported to harbor a large deletion in the TP53 locus and carry an activating CTNNB1 mutation. Furthermore, NCI-H295 cells and their sub-strains have been shown to produce steroids under basal conditions. For decades, the only cell lines available were NCI-H295 and its subclones [86, 87].

The first metastasis-derived ACC cell line MUC-1 was established in 2016. MUC-1 cells represent a preclinical model of EDP-M resistance, as they were obtained from a male patient in progression after EDP-M. MUC-1 cells are characterized by a low steroidogenic activity and by a somatic deletion/frameshift mutation in TP53 gene. Two other metastasis-derived ACC cell lines were subsequently established in 2018, both derived from female patients, namely CU-ACC1 and CU-ACC2. CU-ACC1 cell line secretes high levels of cortisol but not aldosterone, and it is endowed with an activating point mutation of the CTNNB1 gene. CU-ACC2 cells secrete very low amounts of cortisol and carry a mutation in TP53. Another recently available ACC cell model is the JIL-2266 cell line, derived from a female patient with primary ACC and first reported in 2021. JIL-2266 cells are characterized by intermediate-to low expression of SF-1 and their hormone production depends on the composition of the culture medium. Genetically, JIL-2266 cells carry a hemizygous stop-gain mutation in the TP53 gene. Furthermore, a pathogenic germline mutation in the MUTYH gene was observed, leading to the inactivation of the base excision repair process and, consequently, to a high TMB, which characterizes this cell line [86, 87].

The most recent ACC cell line, named TVBF-7 cells, was developed by our group and reported in 2022, established from a perirenal lymph node metastasis of a male ACC patient in progression after EDP-M treatment. TVBF-7 cells produce high levels of cortisol under basal conditions. Genetic analysis reported an altered Wnt/β-catenin pathway, due to the presence of a nonsense APC mutation [86, 87]. Part of the development and characterization of this line is the subject of this PhD project.

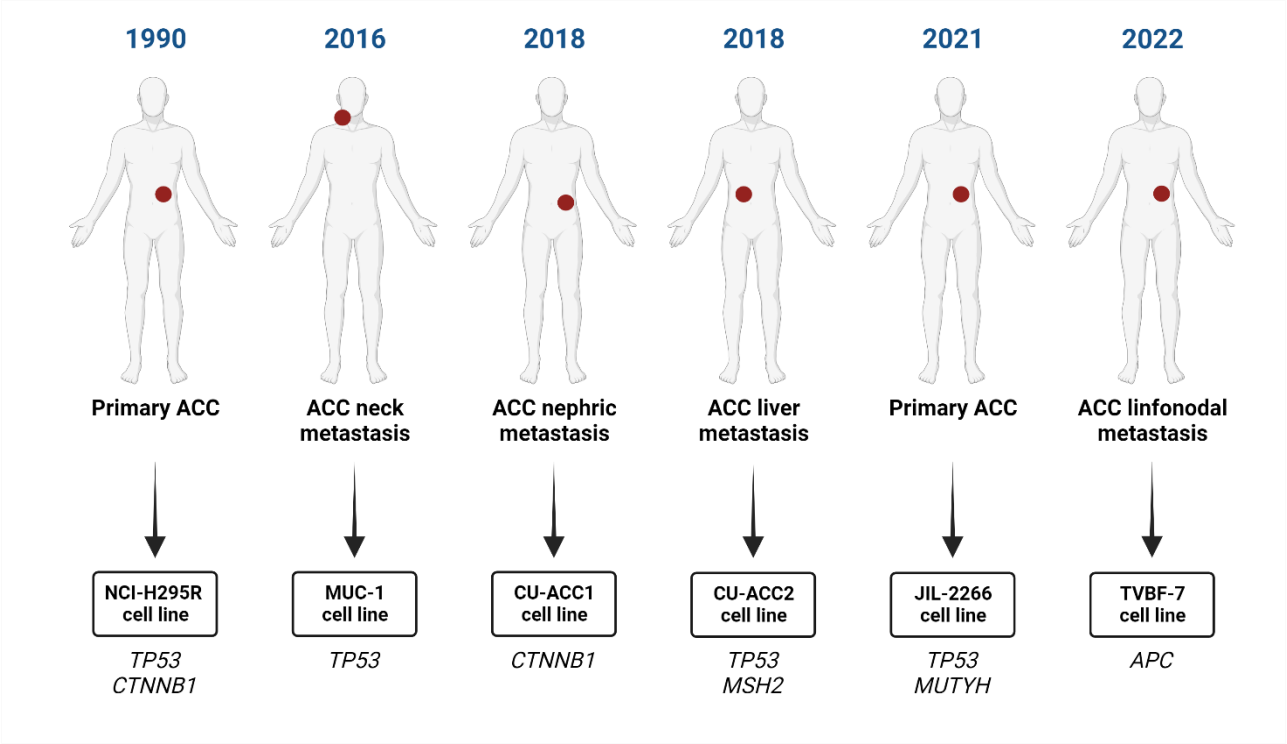

Figure 1.5 Human adult ACC cell lines. The scheme indicates the origin, the year of the first publication in the literature with the new cell model and the genes that are currently known to be mutated.

2 Aim of the PhD project

ACC is a rare tumor characterized by an aggressive behavior. The current pharmacotherapy is based on the adrenolytic drugs mitotane as adjuvant therapy in radically operated patients who are at high risk of relapse. Further, mitotane, combined with the chemotherapeutic drugs etoposide (E), doxorubicin (D), and cisplatin (C) is administered in advanced/metastatic ACC patients not eligible for surgery (EDP-M approach) [18, 58]. However, progression after EDP-M very often occurs and to date there are no standardized and effective further treatment lines [62]. The identification of new pharmacological strategies, particularly in the context of advanced ACC, is thus an urgent need. The aim of my PhD project was to investigate different pharmacological preclinical and translational approaches that could help to respond to this need.

Based on the experimental evidence obtained by our laboratory in past years, I focused my attention on two drugs currently used in clinical practice for other oncological pathologies and characterized by different pharmacological profiles. The first drug, ribociclib, is a drug that targets CDK4/6 as an inhibitor [63]. The second drug, trabectedin, is a DNA-binding agent with a complex mechanism of action [79]. The choice to investigate the effect in ACC of drugs already used in clinics and whose safety profile is already known is an advantage for research in a rare disease such as ACC, although the safety profile is established on patients affected by other diseases; however, it is known that the development of an orphan drug is often not an easily pursued option. Furthermore, the aim of my project is to evaluate as well whether ribociclib and trabectedin could be used in combination with mitotane or with other drugs, such as progesterone, that demonstrate a cytotoxic and antiproliferative effects in both *in vitro* and *in vivo* preclinical models of ACC.

Both drugs were tested not only in traditional cell lines but also in a new human ACC cell line we established in our lab. This new cell line has been developed from a tissue sample of a patient with an ACC metastatic disease underwent surgery.

3 Materials and Methods

3.1 ACC cell model

Each cell line was periodically tested for mycoplasma and authenticated using Short Tandem Repeats profile by BMR Genomics srl (Padova, Italy). Media and supplements were purchased from Merck (Milan, Italy), Thermo-Fisher Scientific (Milan, Italy).

3.1.1 Patient-derived primary culture

ACC115m primary cell culture derived from a patient diagnosed with ACC underwent surgical resection. Cells were established from a lymph-node localization in a male patient underwent disease progression after the EDP-M. The collection of biological samples was approved by the Ethics Committee and informed consent was received from the patient. Tumor tissue was dissociated with gentleMACS^{TM} Dissociator with Tumor Dissociation Kit (Miltenyi biotec, Bologna, Italy). Tumor cells were purified from cells of other origin using the Tumor Isolation Kit (Miltenyi Biotec). Briefly, non-tumor cells were magnetically labeled with a cocktail of antibodies conjugated with MACS^{TM} microbeads, then the cell suspension was loaded onto a MACS column in the MACS separator. The magnetically labeled non-tumor cells were retained within the column, while the tumor cells were collected. Both fractions were cultured in advanced D-MEM/F12, 10% FBS, 1% penicillin-streptomycin, 1% amphotericin B and 2 mM glutamine. To assess the adrenal origin, primary cell cultures were then characterized, evaluating the SF-1 expression by qRT-PCR and by immunofluorescence, as described below. The growing primary culture ACC115m proved to be stable across passages, characterized and subsequently recognized as a new cell line, named TVBF-7 cells [88].

3.1.2 Cell lines

Human NCI-H295R cells were established from a female patient with a primary secreting ACC, and it represents the most widely used experimental cell model to study ACC *in vitro* [86, 89]. MUC-1 cells were derived from a neck metastasis of an EDP-M treated male patient [90]. NCI-H295R cells were purchased from ATCC (American Type Culture Collection, U.S.A.) and maintained in culture according to the ATCC instructions. MUC-1 cells were kindly provided by Dr. Hantel and cultured as indicated in [90].

3.2 Chemicals

Ribociclib succinate was kindly given by Novartis Pharma S.p.A., dissolved in dimethyl sulfoxide (DMSO) and a stock solution of 18mM were prepared, aliquoted and stored at -80°C. Progesterone (Merk, Milano, Italy) was dissolved in DMSO in a stock solution of 100mM, aliquoted and stored at -20°C. Mitotane (Selleckchem Chemicals, DBA Italia, Segrate, Milano, Italy) was dissolved in DMSO in a stock solution of 180mM, aliquoted and stored at -80°C. Trabectedin was kindly given by Pharma Mar S.A. (Madrid, Spain), dissolved in DMSO, and stored at –20 °C in 10 mM aliquots. Cimetidine was purchased from Sigma Aldrich (Sigma Italia, Milano, Italy), resuspended in DMSO, and stored at –20 °C in 10 mM aliquots. For LC-MS/MS experiments drugs were subsequently diluted in methanol, purchased from Carlo Erba Reagents S.r.l. (Milan, Italy).

3.3 Cell treatment

The length of treatment was chosen based on doubling time calculation, according to the ATCC method. In particular, the cells were treated for a time corresponding to approximately 2x doubling time.

3.3.1 Evaluation of the effect of ribociclib alone or combined with progesterone and/or mitotane

Single drug cell-treatment: ribociclib

NCI-H295R cells ($3x10^4$ cells/well), MUC-1 and TVBF-7 (ACC115m) cells ($2x10^4$cells/well) were seeded in 24-wells plates and treated with increasing concentrations of ribociclib. NCI-H295R cell lines and TVBF-7 (ACC115m) primary culture were exposed to ribociclib (2.5 – 100 µM and 2.5 – 75 µM respectively) for 96 hours while MUC-1 cells were exposed to ribociclib (2.5 – 100 µM) for 120 hours.

Binary and ternary drug cell-treatment: ribociclib, progesterone and mitotane

Ribociclib and progesterone combination experiments were performed to evaluate their potential interaction on the viability of NCI-H295R and MUC-1 cells as well as on TVBF-7 (ACC115m) cells. Before treatment, for steroid hormonal depletion, complete medium was switched into dextran-treated charcoal stripped serum (CSS) containing medium (CSS medium). Cells were seeded as above described. NCI-H295R, MUC-1 and TVBF-7 (ACC115m) cells were treated for 96, 120 and 96 hours respectively with ribociclib (2.5 – 100µM) and progesterone (3.75 – 150µM) alone or in combination with a fixed ratio (ribociclib : progesterone = 1 : 1.5), as recommended for the most efficient data analysis according to the Chou and Talalay method [91]. Cells were analyzed for cell viability using MTT as described below. Data were then converted to fraction affected (Fa, range from 0 to 1 where Fa = 0 indicating 100% of cell viability and Fa = 1 indicating 0% of cell viability) and analyzed using the CompuSyn software (ComboSyn inc. Paramus, NJ, USA) to calculate the combination index. The Combination Index < 0.9 being an indication of synergism, Combination Index = 09–1.1 an indication of additive effect, and Combination Index > 1.1 an indication of antagonism. A different approach of binary combination experiment was also used in NCI-H295R and MUC-1 cells. Cells were treated with increasing concentrations of progesterone alone or combined with a fixed concentration of ribociclib. For the ternary treatments, NCI-H295R cells were

seeded as above described and treated with three different concentrations (corresponding to 0.5xIC_{50}, IC_{50} and 2xIC_{50} values) of ribociclib, progesterone and mitotane alone or in combination for 96 hours. Before treatment, the complete medium was switched into CSS-medium.

3.3.2 Evaluation of the effect of trabectedin

Single drug cell-treatment: trabectedin

TVBF-7 cells (2x10^4 cells/well) were seeded in 24-wells plates and treated with increasing concentrations of trabectedin for up to 96 hours (0.0625 – 1.5 nM).

3.4 Cell viability and cell proliferation

Cell viability was evaluated by 3-(4,5-Dimethyl-2-thiazol)-2,5-diphenyl-2H-tetrazolium bromide (MTT) dye reduction assay according to the manufacturer protocol (Merck). Cell proliferation rate was evaluated with TC20 automated cell counter (Bio-Rad Laboratories, Segrate, Italy).

3.5 Gene expression

Gene expression was evaluated by q-RT-PCR (ViiA7, Applied Biosystems, Milan, Italy) and SYBR Green was used as fluorochrome as previously described [92]. Sequences of oligonucleotide primers were listed in Table 3.1. β-actin was chosen as housekeeping gene. Differences in the threshold cycle Ct values between the housekeeping gene and the genes of interest (ΔCt) were calculated as an indicator of the amount of mRNA expressed. The Livak method was applied to analyze the relative changes in gene expression [93].

Table 3.1 Oligonucleotide sequences

Gene	Forward (5' -> 3')	Reverse (5' -> 3')
CDK4	GCCTCGAGATGTATCCTGC	AGTCAGCATTTCCAGCAGCA
CDK6	ATCTCTGGAGTGTTGGCTGC	GGCAACATCTCTAGGCCAGTC
MMP2	ACGACCGCGACAAGAAGTAT	ATTTGTTGCCGAGGAAAGTG
P107	ACGATTCTGCACTGTGGGAG	GTCCCTGCACATTTCCTCCA
P130	CACCCCTCAGATCCAGCAG	CGTGTAGCTTTCGCTCATGC
PgR	CGCGCTCTACCCTGCACTC	TGAATCCGGCCTCAGGTAGTT
Rb	CATCGAATCATGGAATCCCT	GGAAGATTAAGAGGACAAGC
SF1	CAGCCTGGATTTGAAGTTCC	TTCGATGAGCAGGTTGTTGC
TIMP 1	GGGACACCAGAAGTCAACCA	GGGTTGGAAGCCTTTATAGATC
TIMP 2	AACCGGTCAGTGAGAAGGAA	TCTCAGGCCCTTTGAACATC
β-actin	TCTTCCAGCCTTCCTTCCTG	CAATGCCAGGGTACATGGTG

3.6 Immunofluorescence

For the immunofluorescence assay, cells were grown onto 12 mm poly-L-lysine-coated coverslips and then fixed with Immunofix™ (Bioptica Milano S.p.A, Milan, Italy) for 15 min at 4°C and permeabilized with 20% methanol in PBS/Triton X-100 0.1% for 7 min. Nonspecific binding was blocked by incubation in PBS/Triton X-100 0.1% containing BSA 2% for 45 min. Cells were then incubated overnight at 4 °C with the primary antibody. After extensive washes, the Alexa Fluor488 conjugated secondary antibody and Phalloidin 0.165 μM (Thermo-Fisher Scientific) were applied for 1 hour at room temperature. Primary and secondary antibody are listed in Table 3.2. After rinsing, coverslips were mounted using Vectashied® (Immunological sciences, Rome, Italy) as mounting agent with DAPI. Slides were observed by a LSM 510 Zeiss confocal laser microscope (Carl Zeiss S.p.A., Oberkochen, Germany) equipped with Plan-Apochromat 63x/1.4 numerical aperture oil objective. Images were then reconstructed using Zeiss ZEN 2.3 Imaging Software (Carl

Zeiss S.p.A.). Several fields, randomly chosen, were acquired and analyzed for each experimental condition.

3.7 Measurement of cell apoptosis

NCI-H295R, MUC-1 and TVBF-7 (ACC115m) cells (3 x 10^5 cells/well) were seeded in 6-wells plates in complete medium, 24 hours later cells were treated with ribociclib concentration corresponding to IC_{50} calculated values, for 72 or 96 hours. Cells were collected, washed with ice-cold PBS, resuspended in the binding buffer, and stained with Pacific Blue™ Annexin V/ SYOX™ AADVanced™ (Thermo-Fisher Scientific), according to the manufacturer instructions. Cells were then analyzed using MACSQuant10 cytometer (Miltenyi Biotech), using unlabeled cells as negative control. Quantification of apoptosis was determined by FlowJo™ v10.6.2 software (BD Life Sciences, Franklin Lakes, NJ USA). Annexin V+/SYTOX- and Annexin V+/SYTOX+ cells were considered as early and late phase apoptotic cells, according to the manufacturer instructions.

3.8 Cell cycle analysis

Flow cytometric cell cycle analysis was performed as described [94], with minor modifications. Briefly, untreated and ribociclib-treated NCI-H295R, MUC-1 and TVBF-7 (ACC115m) cells were fixed, treated with RNase A (12.5 μg/mL) (Thermo-Fisher Scientific), stained with propidium iodide (40 μg/mL) (Sigma Aldrich Italia) and analyzed by flow cytometry using a MACS Quant Analyzer (Miltenyi Biotec) for cell cycle status. Data were analyzed using FlowJo™ v10.6.2.

3.9 Invasion assay

The *in vitro* invasiveness of cells was evaluated using ECMatrix Cell Invasion Assay™ (Merck). Cells were seeded in culture dish at an appropriate cell density. After 24 hours, cells were

exposed to trabectedin or vehicle in fresh medium for the appropriate time of treatment, determined for each cell line, as above described. Then, cells were detached using trypsin/EDTAand added to the inserts according to manufacturer protocol. Invasive cells were stained after 72 hours of incubation and after washing, inserts were air-dried. Images were acquired using an Olympus IX51 optical microscope (Olympus Italia, Segrate, Italy) equipped with 10x objective. Subsequently, staining was eluted, and absorbance was detected using an EnSight Multimode Plate Reader (PerkinElmer Italia, Milan, Italy) at 560nm.

3.10 Western blot

The conditioned medium from each experimental condition was obtained as described in [95], stored at -80°C for at least 24 hours, resuspended in PBS and the total protein concentration was determined by Bio-Rad Protein Assay (Bio-Rad Laboratories, Segrate, Italy). Proteins were separated by electrophoresis on a 4–12% NuPAGE bis-tris gel system (Thermo-Fisher Scientific) and electroblotted to a polyvinylidene difluoride (PVDF) membrane, incubated with anti-MMP2 (final concentration: 0.9 μg/mL Proteintech, Rosemont, IL, USA) primary antibody. Secondary HRP-labeled anti-rabbit antibody was used, and the signal was visualized using Odyssey® Imaging System (LI-COR Biosciences, NE, USA). Primary and secondary antibody are listed in Table 3.2.

Table 3.2 Primary and secondary antibodies

Target	Characteristic	Company	Final concentration
MMP2	pAb	Proteintech (Segrate, Italy)	0.9 μg/mL
SF-1	Rabbit mAb	Cell Signaling Technologies (Milan, Italy)	0.234 μg/mL
Secondary anti-rabbit	HRP-labeled	Promega Italia (Milan, Italy)	0.4 μg/mL
Secondary anti-rabbit	Alexa Fuor 488 Conjugated	Immunological Sciences (Rome, Italy)	5 μg/mL

3.11 Zymography

Different aliquots of the same conditioned medium samples were used for both western blot and zymography. Proteins were separated by electrophoresis on a 7.5% sodium dodecyl sulfate (SDS)-PAGE gel. Subsequently, gel was incubated for 1 hour with 2.5% Triton X-100 solution at room temperature. Gel was incubated overnight a 37°C with collagenase buffer (NaCl 11.68 g/L, $CaCl_2$,1.47 g/L, Tris 4.84 g/L and Brij® 35 0.06% v/v, brought to pH 7.5). Next, gel was stained with a 0.5% Coomassie R-250 solution (50% water, 40% methanol and 10% acetic acid) for 1 hour and then a decoloring step was performed for 5 minutes with a solution with the same composition without dye. Reagents for buffer and solution preparation were purchased from Merck.

3.12 Fish maintenance and egg collection

Zebrafish were handled according to national and international guidelines (EU Directive 2010/63/EU), following protocols approved by the local committee (Organismo Preposto al Benessere Animale (OPBA), Università degli Studi di Brescia, protocol no. 211B5.24) and authorized by the Ministry of Health (authorization no. 393/2017-PR). The experiments were performed in compliance with the ARRIVE guidelines (https://arriveguidelines.org). Fish were maintained under standard laboratory conditions as indicated [96] particularly at 28°C on a constant 14-hours light/10-hours dark cycle. Fish were fed thrice a day with granular dry food and fresh artemia (Special Diet Services, SDS Diets; LBS Biotech, Horley, UK). Healthy adult wild-type zebrafish (AB) and Tg(kdrl:GFP) zebrafish were used for egg production. The developing embryos were incubated at 28°C and maintained in 0.003% (w/v) 1-phenyl-2-thiourea (PTU; Merck) to prevent pigmentation.

3.13 ACC cell xenograft

ACC cells were exposed overnight with the vital red fluorescent dye CellTrackerTM CM-DiI (Thermo-Fisher Scientific), according to manufacturer protocol. Cells were detached with

trypsin/EDTA, washed in PBS, resuspended in 50 µL of PBS, and kept at 4°C until use. Cell xenografts were performed as described in [97] with minor modifications. Briefly, zebrafish embryos at 48 hours post fertilization (hpf) were dechorionated, anesthetized with 0.042 mg/mL tricaine (Merck), and microinjected with the labeled ACC cells into the subperidermal space of the yolk sac. Microinjections were performed with a FemtoJet electronic microinjector coupled with an InjectMan N12 manipulator (Eppendorf Italia, Milan, Italy). Approximately 250 cells/4 nL were injected into each embryo; embryos were maintained in PTU/fish water in a 32°C incubator. Trabectedin (15 nM) or vehicle were directly added to the PTU/fish water in respectively treated and untreated experimental groups 3 hours after cells injection. Pictures of injected embryos were acquired using Zeiss Axiozoom V13 (Carl Zeiss AG, Oberkochen, Germany) fluorescence microscope, equipped with Zen pro software, 2 hours (T0) and 3 days (T3) after cell injection. The tumor areas of treated and untreated groups at T0 and T3 were measured with Noldus DanioScopeTM software (Noldus Information Technology). Representative embryos at T3 stage were fixed, embedded in low melting agarose, and acquired using a Zeiss LSM 510 META confocal laser-scanning microscope (Carl Zeiss AG) equipped with a 10x objective.

3.14 Quantification of trabectedin uptake in zebrafish embryos

Trabectedin absorption from embryos was evaluated by quantifying the concentration of trabectedin by LC-MS/MS. Ultra-performance liquid chromatography (UPLC) was performed using a DionexTM UltiMateTM 3000 (Thermo-Fisher Scientific) equipped with a LPG-3400SD quaternary analytical pump, a WPS-3000SL analytical autosampler, a TCC-3000SD thermostated column compartment. Chromatographic separation was performed using an Eclipse Plus C18 column (100 mm × 2.1 mm ID, particle size 1.8 µm) (Agilent Technologies, Inc., Milano, Italy). The chromatographic system was set up with a flow rate of 0.150 ml/min. The column was kept at 25°C and equilibrated with 90% mobile phase A (water containing 0.05 % formic acid) and 10% mobile phase B (acetonitrile). The gradient was described Figure 3.1. Reagent-grade acetonitrile for LC-MS

and formic acid (98%) were purchased from Carlo Erba Reagents S.r.l. Ultra-pure water was prepared using a Millipore Milli-Q purification system (Millipore Corporation, Billerica, MA, USA). The UPLC system was coupled with an electrospray ionization mass spectrometer (LCQ Fleet Ion Trap MSn, Thermo-Fisher Scientific).

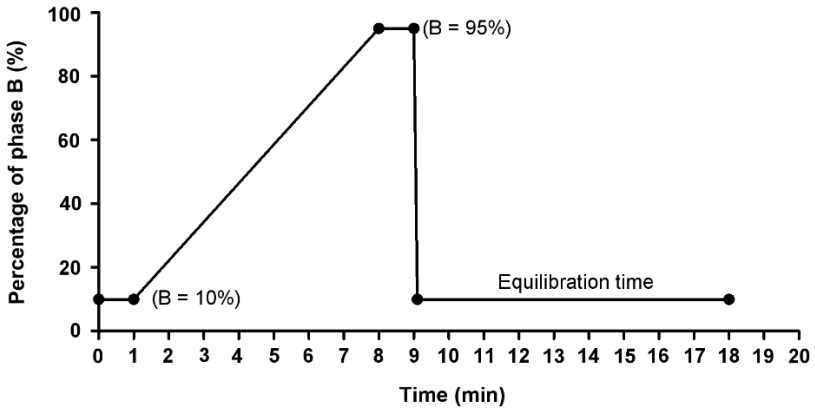

Figure 3.1 Gradient plot of the ultra-performance liquid chromatography (UPLC), presented as percentage of phase B (acetonitrile) vs time.

The positive ESI conditions were set as reported in Table 3.3. Data were treated with the Xcalibur software Version 4.0 (Thermo-Fisher Scientific). The calibration curves for the quantification of trabectedin and cimetidine (used as internal standard (IS) [98]) were obtained both as described below. Fifty embryos for each batch (up to 120 hpf) were put at 4 °C. 100 µL of IS (200 nM) was added to each batch with 100 µL of trabectedin at different dilutions in order to obtain the final concentrations 5-500 nM of trabectedin in methanol. Samples were extracted following the protocol previously reported [97]. 5 µL of each sample were analyzed by LC-MS/MS (LOD 1 nM; LOQ 2.5 nM). The SRM quantified transitions were m/z 744.4 → 495.4 for trabectedin and m/z 253.3 → 156.9 for cimetidine.

Table 3.3 Positive ESI conditions.

Electrospray ionization parameter	**Setting**
Source voltage	5 kV
Source current	100 µA
Capillary voltage	29 kV
Capillary temperature	275°C
Nitrogen sheath gas	15 arb
Auxiliary gas	15 arb
Isolation width	1 mass unit
Range m/z	200-800
Scan time	100 ms
Collision energy (CE)	50%

3.15 Statistical Analysis

Statistical analysis was carried out using GraphPad Prism software version 8 (GraphPad Software, La Jolla, CA, USA). One-way ANOVA with Bonferroni's correction was used for multiple comparisons. Where appropriate, the unpaired t-test was used. Unless otherwise specified, data are expressed as mean ± Standard Error of mean (S.E.M.) of at least three experiments run in triplicate. P values < 0.05 were considered statistically significant.

4 Results

4.1 Establishment of a new ACC cell line

Due to the high heterogeneity of the ACC [99, 100] the preclinical investigation requires different cellular models to test the hypothesis under study in different mutational contexts. For this reason, the development of new cellular models of ACC is of high interest.

The ACC primary culture, identified as ACC115m, was isolated from a lymph node metastasis from a male EDP-M-treated patient without clinically evident signs of steroid excess. No functional testing has been performed. The adrenal origin of these cells was assessed both at mRNA and protein levels. A representative immunofluorescence of SF-1 in ACC115m is shown in Figure 4.1.

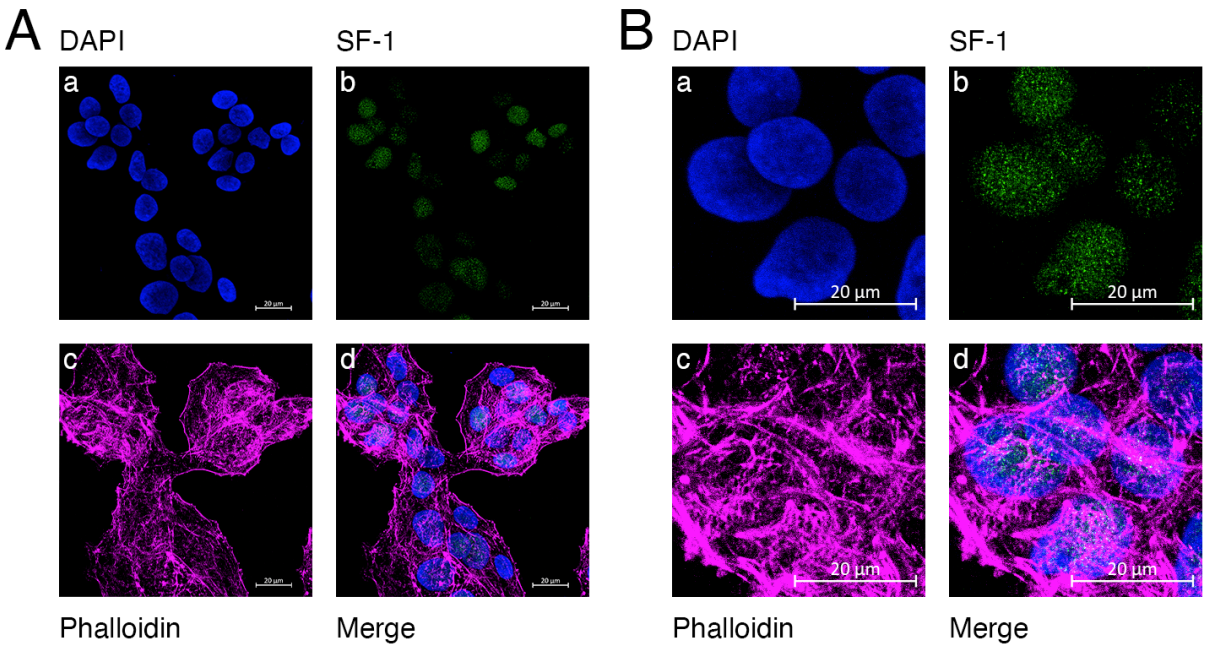

Figure 4.1 ***SF-1 abundance in ACC115m cells evaluated by immunofluorescence. (A)*** *(a) DAPI. (b) SF-1. (c) Phalloidin. (d) Mege all three signals. (B) Cropped area of A. The scale bar is automatically inserted by the software ZEN Black.*

The primary cell culture maintained viability across passages and was stable, as confirmed by cell authentication performed via STR profiling in passages 7, 14, 16, 23, 29 and 49. The STR profile of TVBF-7 cells is reported in Figure 4.2. Moreover, the STR profile of the cells was compared with that of the patient, in order to confirm the origin of the primary culture. Based on the demonstrated stability, the cell model was identified as a novel human ACC cell line, named TVBF-7 cells. An in-depth characterization of TVBF-7 cells was carried out in collaboration with the University of Zurich (Dr. Constanze Hantel). Mutational status revealed a nonsense mutation in APC. Furthermore, endocrinological characterization demonstrated high cortisol secretion [88].

A

MARKER	
AMEL	X
D3S1358	17
D1S1656	16
D2S441	12
D10S1248	14
D13S317	12
PENTA E	5
D16S536	8
D18S51	19
D2S1338	19
CSF1PO	12
PENTA D	9 12
TH01	6
VWA	17
D21S11	29
D7S820	11 12
D5S818	12
TPOX	8
DYS391	--
D8S1179	15
D12S391	18 20
D19S433	13
FGA	21
D22S1045	15

B

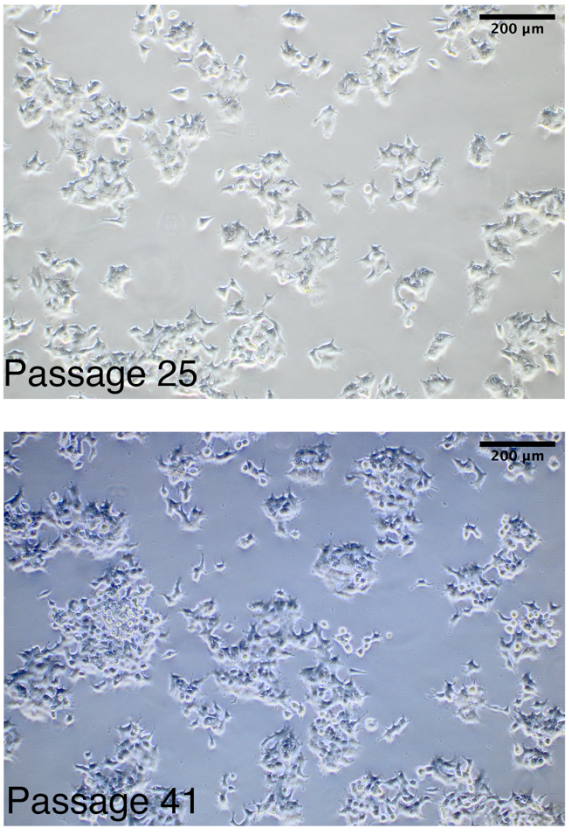

Figure 4.2 TVBF-7: a new ACC cell line. *(A) STR profiling of ACC115m / TVBF-7 cells (B) Brightfield image of TVBF-7 cells acquired at passage 25 and 41. Image was acquired using an Olympus IX51 optical microscope equipped with 10x objective. The scale bar is automatically inserted by the software.*

4.2 Evaluation of the effect of ribociclib in ACC cell models

In this part of the PhD project, I focused my attention on CDK4/6 inhibitor ribociclib. Particularly, we evaluated the effect of ribociclib alone or combined with progesterone and/or mitotane in ACC cell models. The third CDK4/6 inhibitors generation are currently used in the management of advanced HR+, HER2- breast cancer in association with endocrine therapies [101]. Moreover, we previously demonstrate the effect cytotoxic, anti-proliferative and anti-metastatic effect of progesterone in different ACC preclinical models [95, 102-104]. Mitotane was also added as reference drug in ACC [18], to investigate the interplay with the other drugs. Results presented here are part of a published paper [105].

4.2.1 Ribociclib target expression

The expression of ribociclib molecular targets was assessed both in ACC cell lines and in primary cell culture and it revealed an abundant expression of both CDK4 and CDK6 genes in each cell model. Moreover, mRNAs encoding for members of the Pocket Protein Family (Rb, p107, and p130) as targets of the CDK4/6-CiclinD complex, were also assessed. Rb mRNA was highly detected in MUC-1 cell line and in the ACC primary culture, while it was almost undetectable in NCI-H295R cells. mRNA encoding for the Rb-like family proteins P107 and p130 was found expressed in all three cell models, although in different amount. Results are reported in Table 4.1.

Table 4.1 mRNA coding for CDK4, CDK6, Rb, P130 and P107 expression in ACC cells

Cells	CDK4	CDK6	Rb	P130	P107
NCI-H295R	4.30 ± 0.21	6.98 ± 0.04	ND	11.07 ± 0.11	7.86 ± 0.20
MUC-1	6.45 ± 0.12	7.89 ± 0.02	7.89 ± 0.12	9.78 ± 0.03	8.66 ± 0.11
TVBF-7 (ACC115m)	3.50 ± 0.09	6.48 ± 0.05	8.69 ± 0.24	13.11 ± 0.20	12.07 ± 0.10
Results are presented as ΔCt (Ct of β-actin – Ct gene of interest) ± SD					

4.2.2 Ribociclib in ACC cell models: effect on cell viability and cell proliferation

Firstly, we evaluated the effect of ribociclib as a single treatment on ACC cell viability and cell proliferation. Exposure of NCI-H295R cells to increasing concentrations of ribociclib (2.5 – 100 μM) for 96 hours led to a concentration-dependent reduction of cell viability. Sigmoidal concentration-response function was applied to calculate the IC_{50} value of ribociclib, that was 21.60 μM (95% confidence interval [CI]: 18.63-25.04 μM). The highest concentration tested of 100 μM left about 2% of viable cells, indicating the high ribociclib efficacy in this cell line (Figure 4.3A). Ribociclib reduced as well the cell proliferation rate of NCI-H295R cells, as shown in Figure 4.3B. The metastasis-derived cell line MUC-1 was as well responsive to ribociclib (2.5 – 100 μM); indeed, after 120 hours exposure, a concentration dependent decrease of cell viability was observed. The calculated IC_{50} value was 48.16 μM (95%CI: 39.64- 50.13 μM). In this cell line, ribociclib showed a decreased potency compared to NCI-H295R, with a similar efficacy (Figure 4.3A). The effect on the cell proliferation rate was as well evaluated and results reported in Figure 4.3B demonstrated a ribociclib concentration-dependent reduction of the cell number. Ribociclib was also evaluated in TVBF-7 (ACC115m) cells. Exposure of these cells to increasing concentration of ribociclib (2.5 – 75 μM) for 96 hours induced a concentration dependent decrease of cell viability. The calculated IC_{50} value was 46.1 μM (95%CI: 44.56- 47.64 μM). In these cells ribociclib induced an effect on cell viability superimposable to that observed in MUC-1 (Figure 4.3A), accordingly to the origin of both ACC cells from patients underwent progression after EDP-M. The effect on cell proliferation was as well demonstrated (Figure 4.3B).

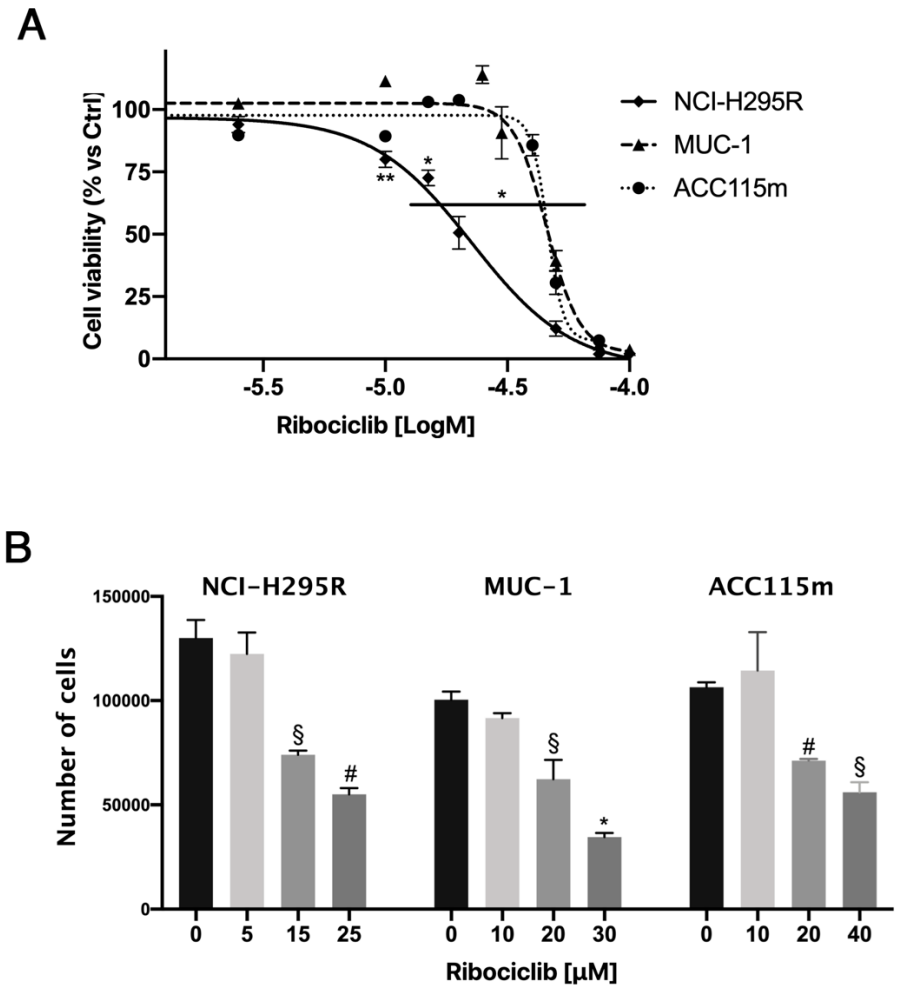

Figure 4.3 Cytotoxic and antiproliferative effect of ribociclib on ACC cell models*. (A) Concentration-response curves ribociclib-induced inhibition of cell viability. NCI-H295R, MUC-1 and ACC115m cells were treated with increasing concentration of ribociclib for 96 hours, 120h and 96 hours 120h and 96 hours respectively. Cell viability was evaluated by MTT assay. (B) Effect of ribociclib on cell proliferation. NCI-H295R, MUC-1 and ACC115m cells were treated with three concentrations of ribociclib for 96 hours, 120h and 96 hours respectively. Cells proliferation was assessed after cells count with trypan blue exclusion Results are expressed as percent of viable cells vs. untreated cells (Ctrl) ± S.E.M. [* $p < 0.0001$; ** $p < 0.001$; # $p < 0.01$; § $p < 0.05$].*

4.2.3 Ribociclib-induced increase of apoptotic cells

To investigate the mechanism of cell death induced by ribociclib in our experimental models, we performed in untreated and ribociclib-treated cells a double staining assay, as described in Material and Methods. Results are reported in Figure 4.4. The exposure of both cell lines and primary cells to a concentration of ribociclib corresponding to the respective IC_{50} values for 96 hours induced an increase in apoptotic cells (NCI-H295R apoptotic cells: untreated cells: 12.0% ± 1.0%; ribociclib-treated cells: 31.0% ± 4.0%; $p < 0.05$. MUC-1 apoptotic cells: untreated cells: 4.5% ± 0.5%; ribociclib-treated cells: 87.5% ± 7.5%; $p < 0.01$. TVBF-7 (ACC115m) apoptotic cells: untreated cells: 19.0% ± 1.0%; ribociclib-treated cells: 83.5% ± 1.5%; $p < 0.001$). The analysis was as well performed after 96 hours of treatment, and results confirm the observed trend (data not shown).

4.2.4 Effect of ribociclib on cell cycle

Ribociclib is known to interfere with the cell cycle progression [106]. To evaluate the effect of ribociclib treatment on the distribution of NCI-H295R and MUC-1 cells in the cell cycle, we performed preliminary time-course evaluation of cell cycle distribution, in order to define the best treatment time for subsequent experiments. Then, cells were exposed to a concentration corresponding to the IC_{50} value of ribociclib for 72 hours and results reported in Figure 4.5 indicated an increase of the cell percentage in G1 phase in ACC115m primary cells (cells in G1 phase: untreated cells: 60.8% ± 3.0%; ribociclib-treated cells: 75.5% ± 1.9%; $p < 0.01$) while an increase in G2 phase was observed in both NCI-H295R (cells in G2 phase: untreated cells: 26.0% ± 2.0%; ribociclib-treated cells: 35.1% ± 0.9%; $p < 0.05$) and MUC-1 (cells in G2 phase: untreated cells: 23.6% ± 1.4%; ribociclib-treated cells: 44.3% ± 3.0%; $p < 0.01$) cell lines.

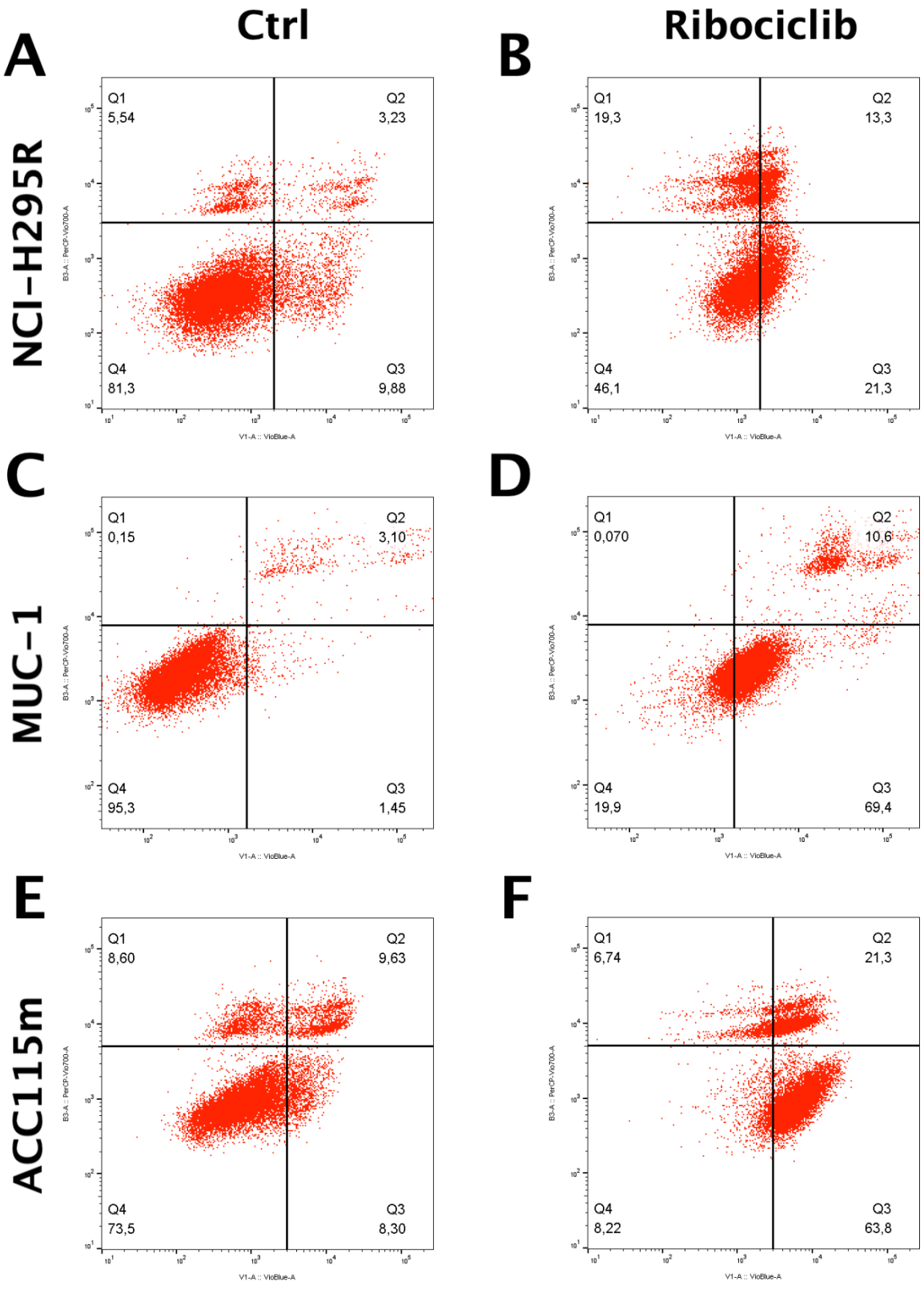

Figure 4.4 Cell apoptosis in ACC cells after 72 hour treatment with ribociclib. *Alive cells are shown in the lower left part of the panel (Q4); early apoptotic cells are shown in the lower right part of the panel (Q3 late apoptotic cells are shown in the higher right part of the panel (Q2); necrotic cells are shown in the higher left part of the panel (Q1). Representative images and data of one out of three experiments are shown.*

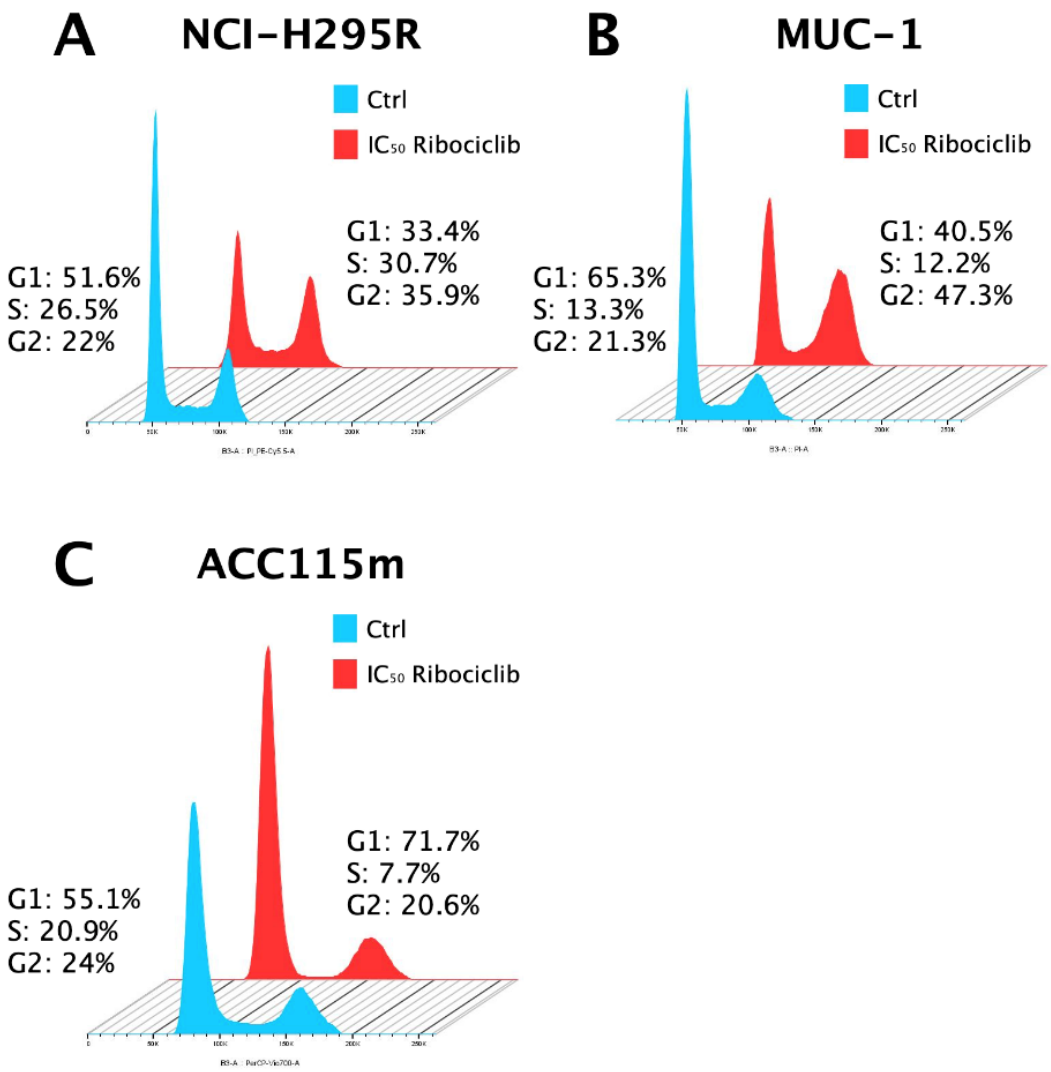

Figure 4.5 Cell cycle analysis after ribociclib-treatment. *DNA histograms. (A) NCI-H295R untreated cells and 3 days ribociclib-treated cells. (B) MUC-1 untreated cells and 3 days ribociclib-treated cells. (C) TVBF-7 (ACC115m) untreated cells and 3 days ribociclib-treated cells. Representative images and data of one out of three experiments are shown.*

4.2.5 Progesterone enhanced the ribociclib effect in ACC cell models

We have already demonstrated the cytotoxic effect of increasing concentrations of progesterone in NCI-H295R cells [102] and in MUC-1 cells [103], with differences in potency and efficacy. Binary combination experiments were then performed, establishing the concentration response curves according to the Chou-Talalay method: NCI-H295R and MUC-1 were treated with ribociclib and progesterone alone or in combination. Cells were exposed to a drug fixed ratio (ribociclib : progesterone = 1 : 1.5). Concentration-response curves of combination experiments were

reported in Figure 4.6A and in Figure 4.6C. Data on cell viability were converted in Fraction Affected (FA) and the Combination Index was calculated with the CompuSyn Software. Figure 4.6B and in Figure 4.6D shows the semilogarithmic-Combination Index Plots. When values of Log(Combination Index) > 0 the effect is antagonist, when Log(Combination Index) $= 0$ and < 0 the effect is additive and synergic, respectively. These results show that at the higher concentrations considered the effect was additive/synergistic in both ACC cell lines. Finally, we evaluate the ribociclib/progesterone combination cytotoxic effect also in the TVBF-7 (ACC115m) cells, that showed a response to the cytotoxic effect of progesterone superimposable to that observed in MUC-1 cells [32]. Cells were indeed treated with ribociclib and progesterone alone or in combination with a fixed ratio of concentrations (ribociclib : progesterone = 1 : 1.5). Concentration-response curves of combination experiments were reported in Figure 4.6E. As reported in Figure 4.6F, the results of the combination index plot indicate a moderate additive/synergistic effect. To investigate whether low concentrations of ribociclib could still positively influence the response of these cells to progesterone, our ACC cell models were treated with increasing concentrations of progesterone alone or combined with a fixed dose of ribociclib. The ribociclib cytotoxic IC_{15} was chosen for each cell lines (NCI-H295R = 10 μM; MUC-1 = 30 μM; TVBF-7-ACC115m = 40 μM). Results are reported in Figure 4.7. The effect in NCI-H295R cells did not differ between the single drug or the combination (Figure 4.7A), while, in MUC-1 cells and in TVBF-7 (ACC115m) cells, the combination of increasing concentrations of progesterone with a low concentration of ribociclib induced an increase in the potency of progesterone (Figure. 4.7B and Figure 4.7C). Indeed, the IC_{50} values of the combination were 45.77 μM (95%CI: 34.99 – 59.87 μM) and 29.60 μM (95%CI: 26.67 – 32.73 μM) in MUC-1 and ACC115m respectively, and they were significantly ($p<0.01$ for both cell models) reduced compared to the IC_{50} values of progesterone alone, that were 67.58 μM (95%CI: 63.44 – 71.98 μM) and 59.52 μM (95%CI: 51.06 – 69.39 μM) for MUC-1 and ACC115m respectively, in line with our previous results [103].

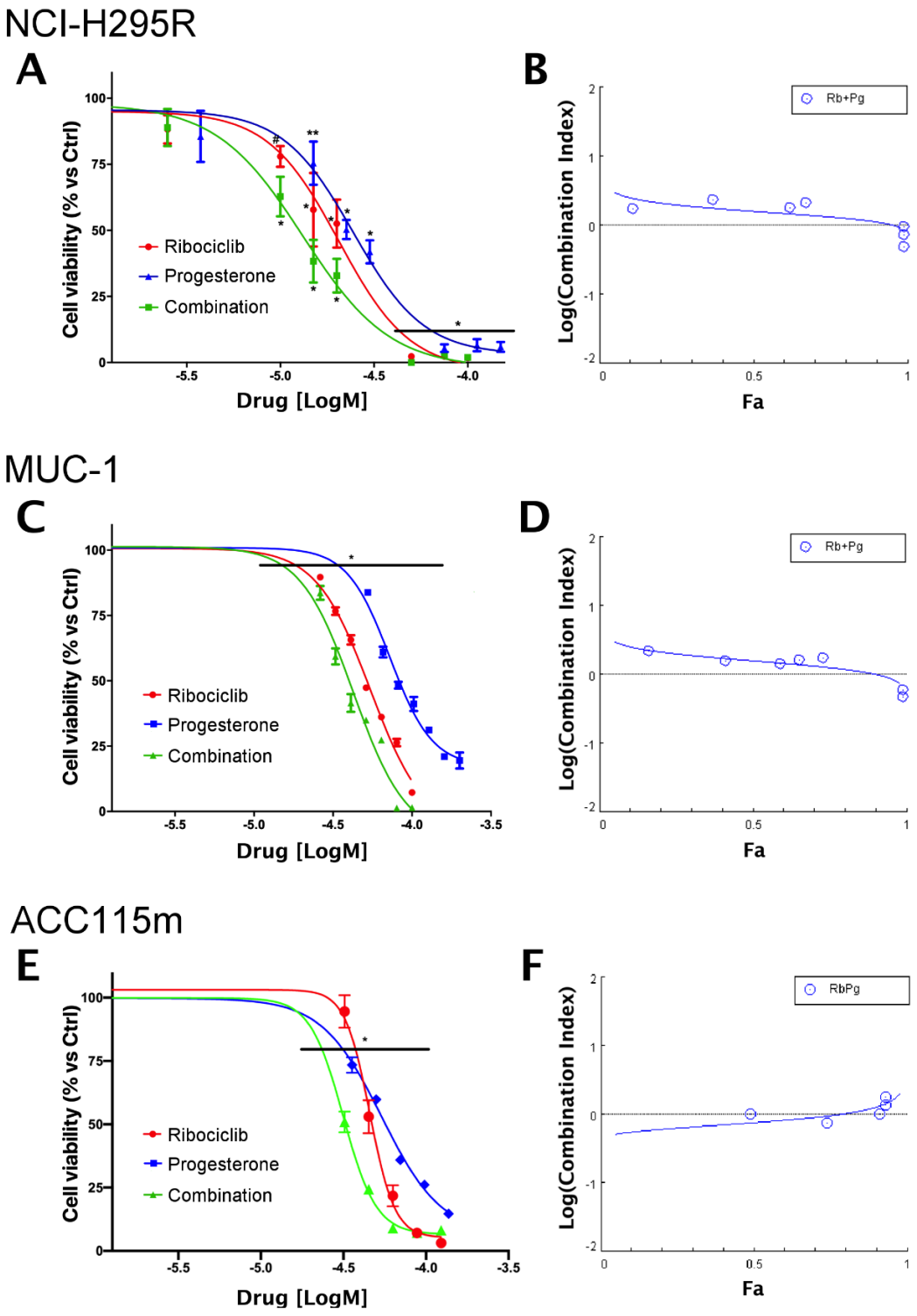

Figure 4.6 Effect of the ribociclib (Rb)/progesterone (Pg) combination on ACC cell models viability. *Cells were exposed to increasing concentrations of ribociclib and progesterone alone or in combination at fixed concentration ribociclib : progesterone = 1 : 1.5 molar ratio. Cell viability was measured by MTT. Concentration–response curves in NCI-H295R cells (A), in MUC-1 cells (C) and in TVBF-7 (ACC115m) cells (E). Results are expressed as percent of viable cells vs. untreated cells (Ctrl) ± S.E.M. (B, D and F) Combination Index plot in NCI-H295R, MUC-1 and TVBF-7 (ACC115m) cells respectively. Dose and effect data obtained were converted to Fa values and analyzed with CompuSyn software. [* $p < 0.0001$; ** $p < 0.001$; # $p < 0.01$].*

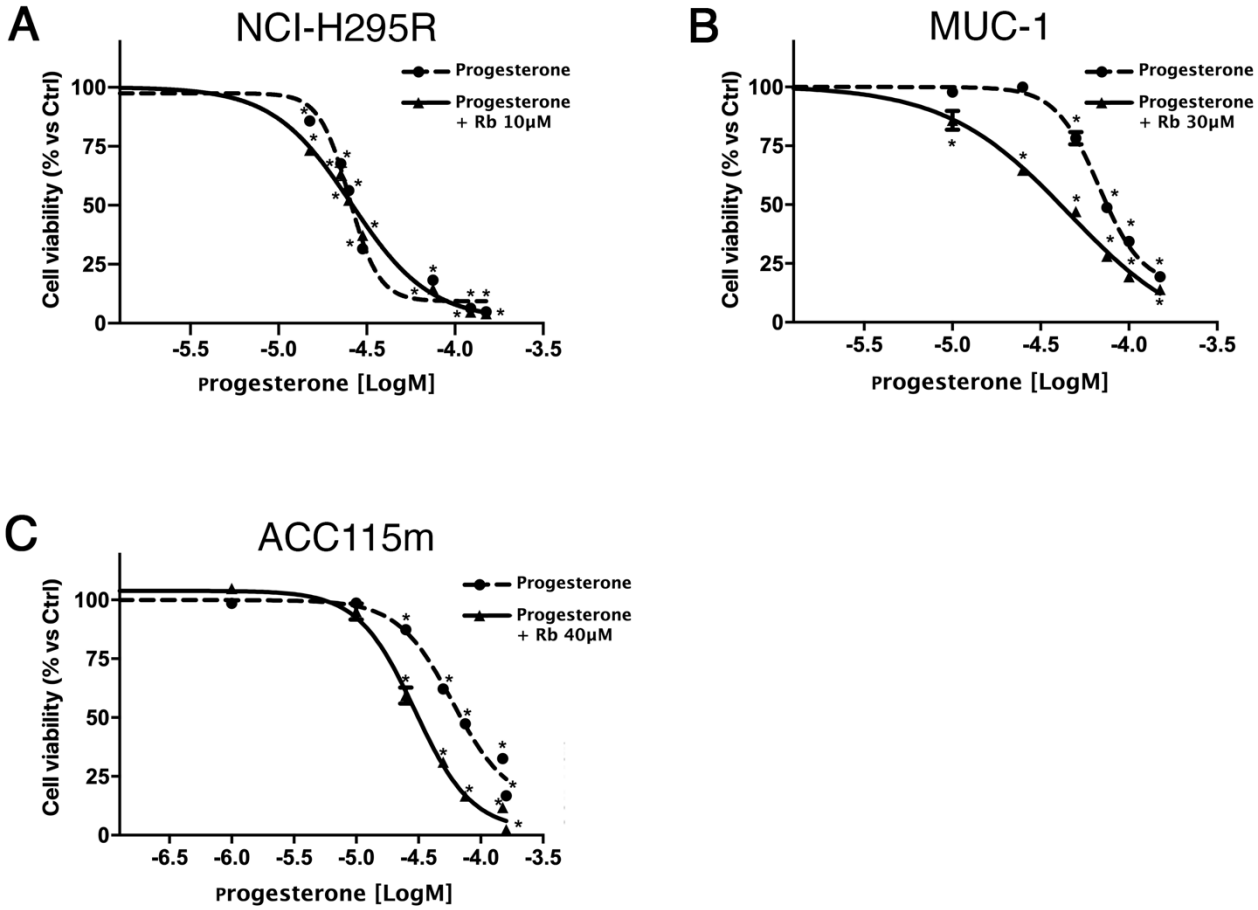

Figure 4.7 Progesterone alone or combined with a fixed dose of ribociclib ACC cell models*. (A) Concentration-response curve in NCI-H295R cells. Cells were treated with increasing concentration of progesterone alone or combined with 10μM of ribociclib for 96 hours. (B) Concentration-response curve in MUC-1 cells. Cells were treated with increasing concentration of progesterone alone or combined with 30μM of ribociclib for 120 hours. (C) Concentration-response curve in TVBF-7 (ACC115m) cells. Cells were treated with increasing concentration of progesterone alone or combined with 40μM of ribociclib for 96 hours. Cell viability was evaluated by MTT. Results are expressed as percent of viable cells vs. untreated cells (Ctrl) ± S.E.M. [* $p < 0.0001$].*

4.2.6 Effect of ternary combination of ribociclib, progesterone and mitotane on NCI-H295R cell viability

The effect of mitotane on NCI-H295R cells is well documented [102, 107]. We then evaluated the response of MUC-1 cells and of TVBF-7 (ACC115m) cells to mitotane treatment (Figure 4.8). MUC-1 cells were responding to mitotane in a high range of concentrations and our results are in line with published literature [108]. According to the origin of this primary culture, derived from a patient

underwent progression under mitotane, TVBF-7 (ACC115m) cells is partially resistant to high concentrations of mitotane.

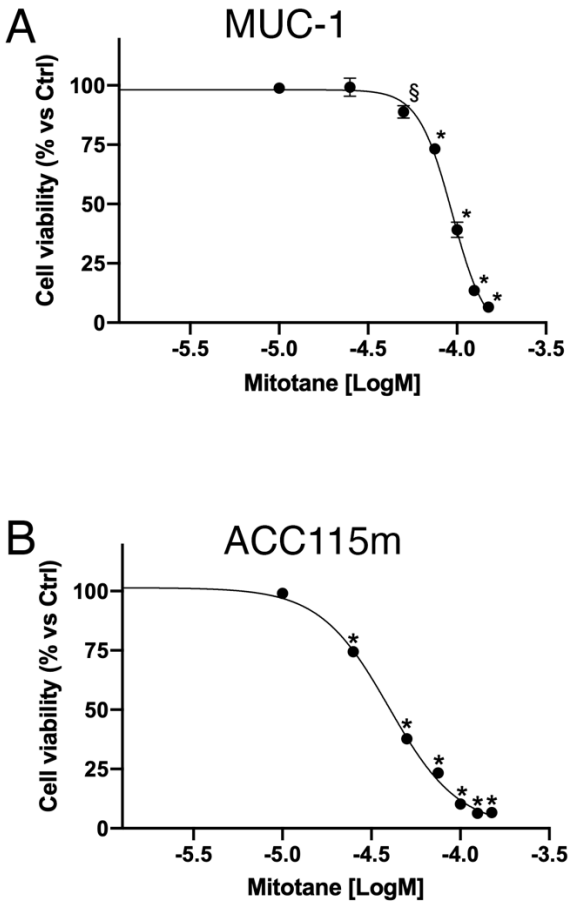

Figure 4.8 Cytotoxic effect of mitotane on (A) MUC-1 cells and (B) ACC115m cells. *Cells were treated with increasing concentrations of mitotane (10 – 150 μM) for 120 and 96 hours respectively. Cell viability was evaluated by MTT ass. Results are expressed as percent of viable cells vs. untreated cells (Ctrl) ± S.E.M. [* p < 0.0001; § p < 0.05].*

Considering the different sensitivity of the ACC cell models to the drugs, all of them were used in order to evaluate the effect on the viability of the ternary treatment. The reduction of cell viability is reported in Figure 4.9. In each ACC cell models, the effect of the combination was more evident for values corresponding to 0.5 x IC_{50} and 1 x IC_{50}, where a greater and statistically significant reduction in the cell viability in the combined treatment, compared to individual treatments was observed.

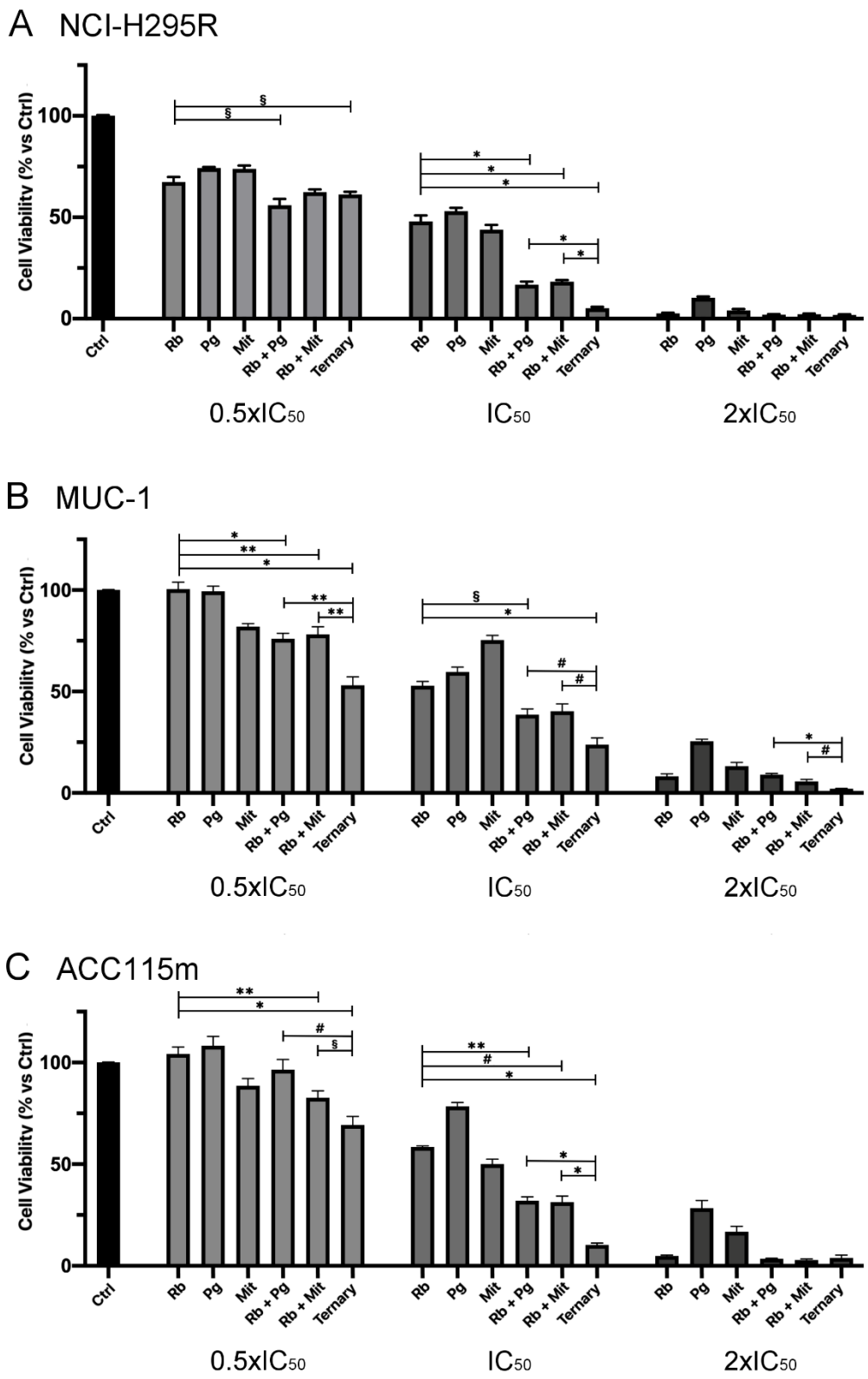

Figure 4.9 Effect of ribociclib, progesterone and mitotane on cell viability in ACC cell models. *(A) NCI-H295R (B) MUC-1 and (C) TVBF-7 (ACC115m) cells were exposed to three concentrations of each drug, corresponding to 0.5x, 1x and 2x IC_{50} values, alone or in ternary combination for 4, 5 and 4 days respectively. Results are expressed as percent of viable cells vs. untreated cells (Ctrl) ± S.E.M. [* $p < 0.0001$; ** $p < 0.001$; # $p < 0.01$; § $p < 0.05$].*

4.3 Evaluation of the effect of trabectedin in ACC preclinical models

We have already demonstrated the *in vitro* long-lasting cytotoxic activity of trabectedin in NCI-H295R and MUC-1 cell lines as well as in ACC primary cultures. Furthermore, we reported a trabectedin-induced β-catenin translocation in NCI-H295R cells [109]. In this part of the PhD project, I focused my attention on the evaluation of the effect of trabectedin on ACC cell invasiveness and metastasis formation, using both cell models and zebrafish embryos xenografted with ACC cells. In this second part of my project, the ACC115m cells were already stabilized, characterized and named TVBF-7 [88]. Thus, in the following results, they are named TVBF-7 cells. Results presented here are part of a published paper [110].

4.3.1 Trabectedin induces cytotoxic and antiproliferative effects in ACC experimental cell models

Trabectedin reduces cell viability in NCI-H295R and MUC-1 cell lines with an IC_{50} of 0.15 nM and 0.8 nM, respectively [109]. Efficacy of trabectedin on the ACC cell line TVBF-7 cells was then evaluated. Exposure of TVBF-7 cells to increasing concentrations of trabectedin (0.0625–1.5 nM) for 96 hours led to a concentration-dependent reduction of cell viability. Sigmoidal concentration-response function was applied to calculate the IC_{50} value of trabectedin, which was 0.68 nM (95% confidence interval (CI): 0.46–1.01nM). The drug was highly active in inducing cytotoxicity, indeed its efficacy reached about 90% at the highest concentration tested (Figure 4.10A). The effect of drug-treatment discontinuation on TVBF-7 cell viability was evaluated as well. Cells were exposed to trabectedin for 96 hours, and then medium was replaced with drug-free medium for additional 96 hours. Results indicated a long-lasting effect of trabectedin also in TVBF-7 cells, as reported in Figure 4.10B.

Trabectedin affected the cell proliferation rate as well. The impact of drug treatment on this process was evaluated in each ACC cell model. NCI-H295R, MUC-1 and TVBF-7 cells were treated

with three concentrations of trabectedin, corresponding to 0.5x, 1x and 2x of the respective IC_{50} trabectedin values obtained with the cytotoxicity experiments. Cell count revealed a concentration-dependent reduction of the cell proliferation rate in each ACC cell model (Figure 4.11). Trabectedin displayed a higher potency in the inhibition of the ACC cell proliferation compared to the cytotoxic effect, in particular the MUC-1 cells seemed to be more sensitive to the antiproliferative effect of trabectedin.

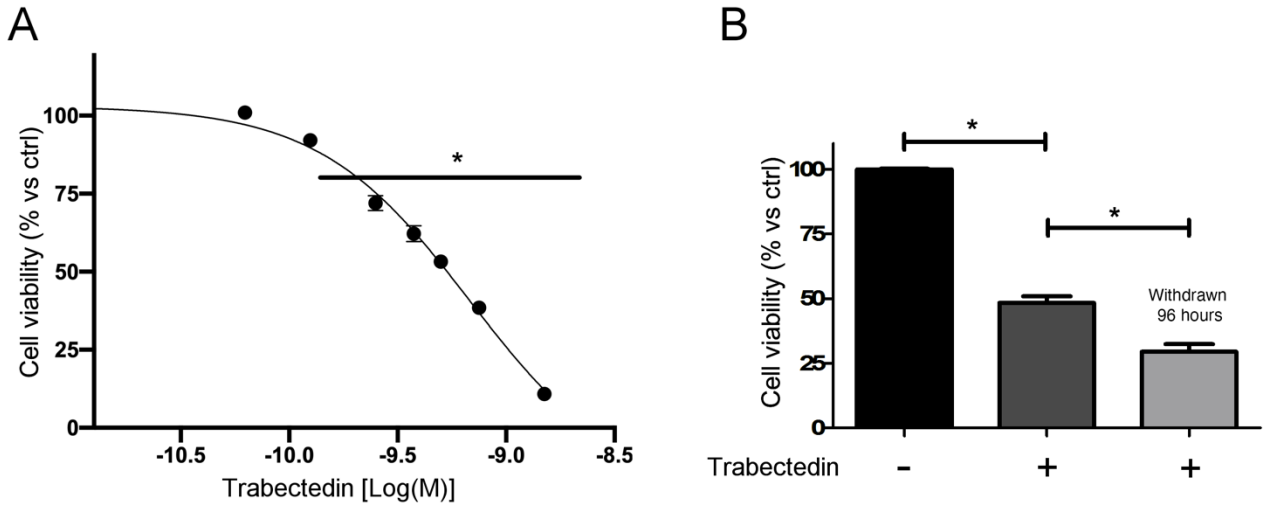

Figure 4.10 Trabectedin impaired TVBF-7 cell viability. *(A) Concentration–response curve of trabectedin-induced inhibition of cell viability. Cells were treated with increasing concentrations of trabectedin (0.0625–1.5 nM) for 4 days. (B) Cytotoxic effect lasted after trabectedin withdrawn. Cells were treated with the trabectedin IC_{50} (0.68 nM) for 96 hours, then trabectedin was withdrawn from medium, and cells were kept in culture for a further 96 hours. Cell viability was evaluated by MTT assay. Results are expressed as percent of viable cells vs untreated cells ± SEM. *P < 0.0001.*

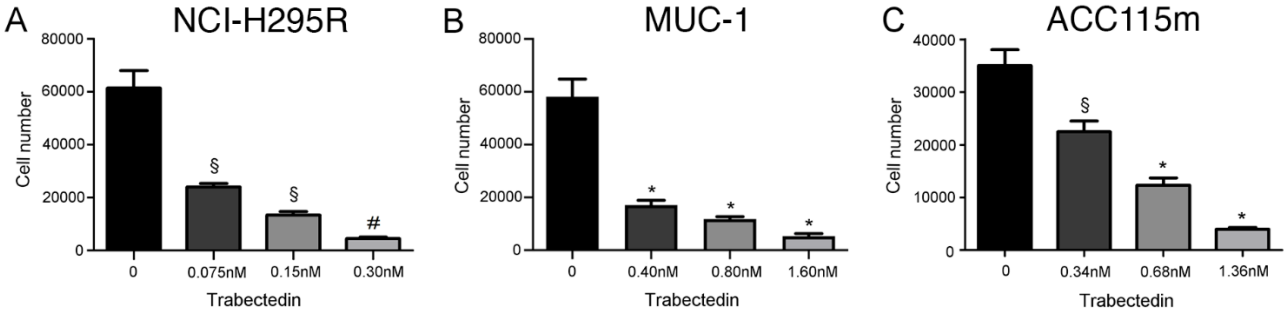

Figure 4.11 Effect of trabectedin on ACC cell proliferation*. (A) NCI-H295R (B) MUC-1 (C) TVBF-7 cells were treated for 96, 120, 96 hours respectively with 0.5x, 1x and 2x IC_{50} values of cytotoxic effect of trabectedin. Cell proliferation was assessed by cell count with trypan blue exclusion. Viable cell numbers are expressed as mean ± SEM. *P < 0.0001; # P < 0.001; §P < 0.01.*

4.3.2 Trabectedin induced a reduction of ACC cell xenograft area and metastasis formation in zebrafish embryos

The effect of trabectedin on cell proliferation and cytotoxicity was then evaluated in an *in vivo* preclinical model using zebrafish embryos xenografted with ACC cells and randomly assigned to be exposed to vehicle or to 15nM of trabectedin. Trabectedin concentration was chosen accordingly to preliminary experiments aimed to evaluating the concentration of drug in the embryos. LC-MS/MS analysis revealed that trabectedin is adsorbed by the embryos. In particular, the concentration (± SD) of trabectedin in embryos exposed to 15nM of trabectedin dissolved in fish water for 72 hours was 0.22nM ± 0.05nM. Trabectedin induced a statistically significant reduction of cell xenograft area compared to vehicle for each experimental cell model, as reported in Figure 4.12A. Figure 4.12B shows representative figures of Tg(kdrl:GFP) zebrafish embryos xenografted with the three cell lines and exposed to vehicle or trabectedin.

As MUC-1 and TVBF-7 cells derive from ACC metastatic localizations, we then investigated whether these cell lines retain the ability to migrate from the embryo injection site. The presence of metastasis (defined as cells at sites other than injection site) at T3 was evaluated. MUC-1 cells were found to be able to metastasize in the tail of the embryos. Trabectedin exposure reduced the percentage of metastases-positive embryos xenografted with MUC-1 cells treated from (mean ± SD) 72.15% ± 9.65% to 24.20% ± 3.52% ($p < 0.01$). TVBF-7 cells were found to be able to form metastases as well, although at lower rate. Indeed, metastases were observed in the pericardial area and the percentage of metastases-positive embryos was 12.07% ± 7.31% in vehicle-exposed embryos and 1.19% ± 2.06% in trabectedin-treated embryos, although the reduction did not reach a statistical significance. Figure 4.13 showed a representative image of MUC-1 and TVBF-7 metastatic cells. No metastases were observed in embryos xenografted with NCI-H295R cells, in line with their primary ACC origin.

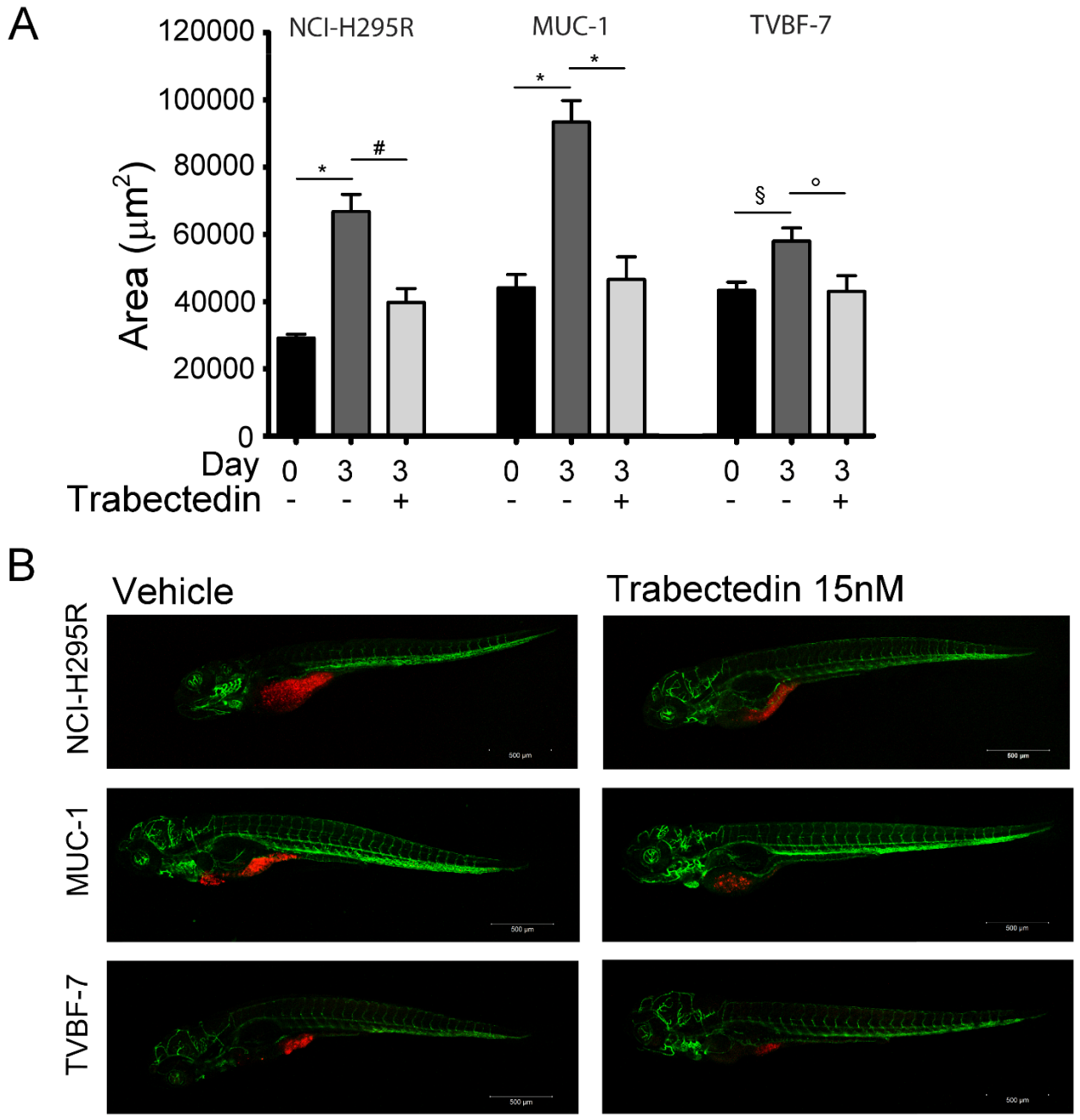

Figure 4.12 Trabectedin induced a reduction of the tumor xenograft area of ACC cells*. (A) Tumor areas of 48 hpf (T0 - start of treatment) and 120 hpf (T3 – end of treatment) of drug-treated and vehicle-treated groups were measured with Noldus DanioScopeTM software. (B) Representative images of 120 hpf trabectedin-treated and vehicle-treated embryos are shown. Each ACC cell line was labeled with a red fluorescent lipophilic dye while the embryo endothelium was labeled with a green fluorescent protein reporter driven by the kdrl promoter. Images were acquired using a Zeiss LSM 510 META confocal laser-scanning microscope equipped with a 10x objective. Data are shown as mean ± SEM. *P < 0.0001; # P < 0.001; §P < 0.01; ° P < 0.05.*

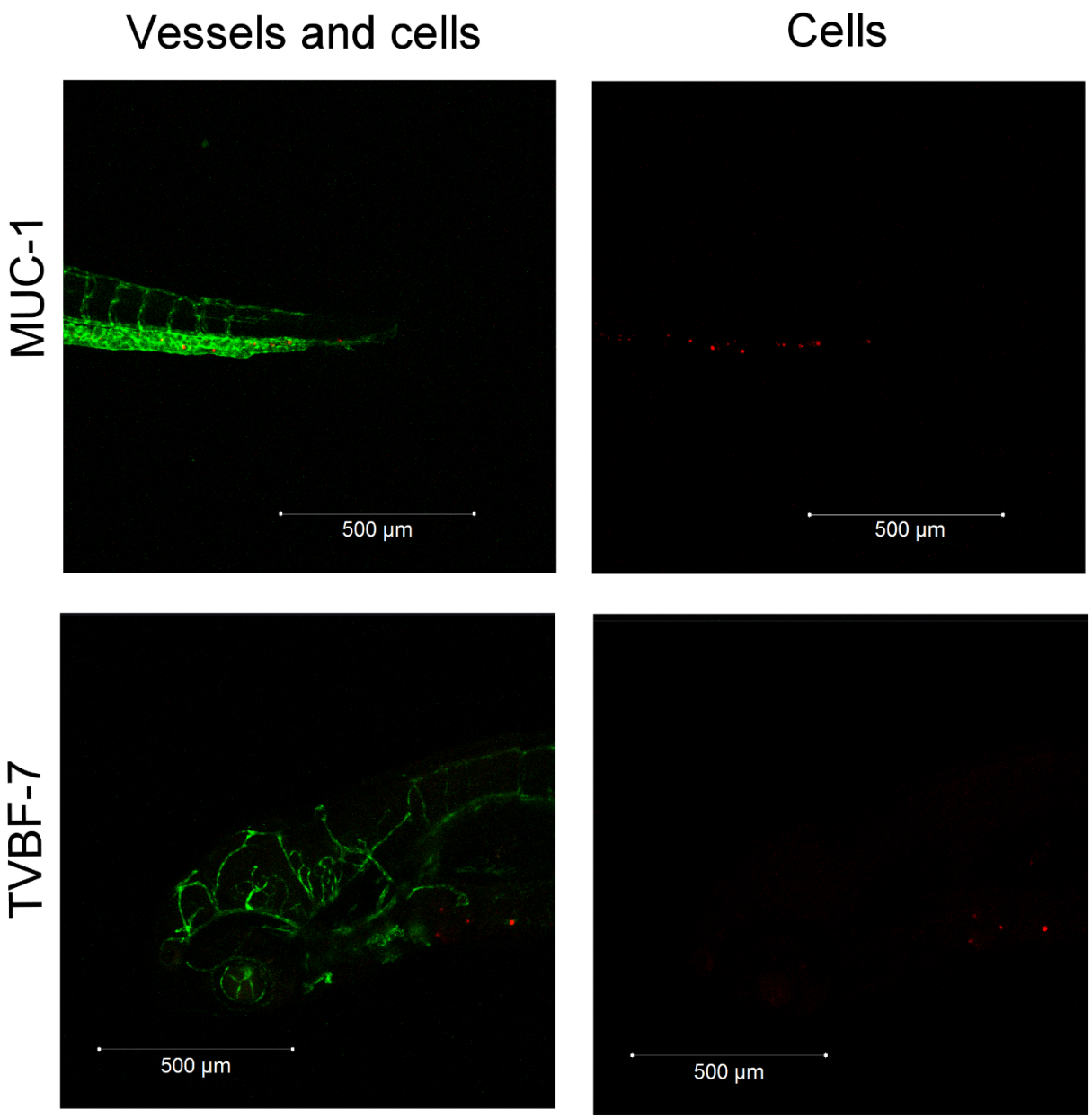

Figure 4.13 MUC-1 and TVBF-7 ACC cells induced metastasis formation in zebrafish embryos. *In the upper panels a representative acquisition of the metastases of MUC-1 cells in the tail of the embryo is shown. In the lower panels a representative acquisition of the metastases of TVBF-7 cells in the pericardial area of the embryo is shown. Images were acquired at 120 hpf using a Zeiss LSM 510 META confocal laser-scanning microscope equipped with a 10x objective.*

4.3.3 Trabectedin reduced cell invasiveness

Results obtained in the zebrafish embryo model were then confirmed and deepen with an *in vitro* approach, studying the invasiveness capability of the ACC cell models. NCI-H295R, MUC-1 and TVBF-7 cells were exposed to their respective trabectedin IC_{50} values. As shown in Figure 4.14A, trabectedin treatment significantly reduced the invasiveness through the matrix of both cell lines established from patients in progression after EDP-M, as MUC-1 cells (untreated: mean OD ± SD = 0.390 ± 0.029; trabectedin-treated: 0.114 ± 0.014, p = 0.0070) and TVBF-7 cells (untreated: 0.319 ± 0.062; trabectedin-treated: 0.210 ± 0.034, p = 0.029). NCI-H295R cells displayed a low invasiveness capability, accordingly to their origin, that was not significantly modified by trabectedin treatment (untreated: 0.134 ± 0.039; trabectedin-treated: 0.079 ± 0.008, ns). Figure 4.14B shows a representative image of the Cell Invasion Assay.

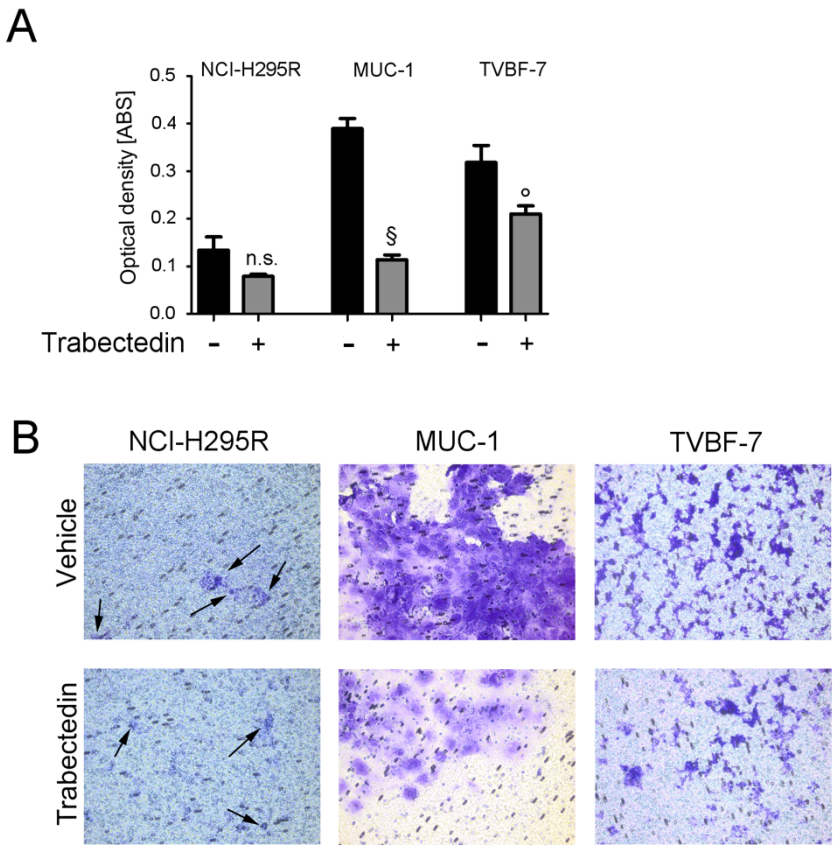

Figure 4.14 Trabectedin impaired the in vitro invasion ability of ACC cells. *(A) Quantification of invasive cells after 72 hours of incubation. The absorbance of the staining was detected at 560nm. Each point was run three times in triplicate. (B) Representative images of ACC invasive cells after 72 hours of incubation. Black arrows indicate invasive NCI-H295R cells. Images were acquired using an Olympus IX51 optical microscope equipped with 10x objective.* § $P < 0.01$; ° $P < 0.05$.

4.3.4 Trabectedin affects metalloprotease 2 (MMP2) activity in metastatic ACC cell lines.

It is known that matrix metalloproteinase type 2 (MMP2) is involved in metastases processes in the context of ACC [111]. To investigate whether trabectedin could reduce the *in vitro* and *in vivo* invasiveness of metastatic ACC cell models through the modulation of MMP2 expression/activity, the MMP-2 as well as its inhibitors TIMP1 and TIMP2 gene expression were firstly evaluated in vehicle-treated and trabectedin-treated cells. Results demonstrated a low, not significant reduction in MMP2 gene expression (MUC-1: $\Delta\Delta Ct = 0.815$; TVBF-7: $\Delta\Delta Ct = 0.261$). Measuring the gene expression of the tissue inhibitors of MMP-2, namely TIMP-1 and TIMP-2 and a low, not significant increase in TIMP-2 gene expression (MUC-1: $\Delta\Delta Ct = -0.85$; TVBF-7: $\Delta\Delta Ct = -0.03$) was observed, while a significant increase in gene expression was, however, observed for TIMP1 in both cell models (MUC-1: $\Delta\Delta Ct = -2.00$; TVBF-7: $\Delta\Delta Ct = -1.75$).

MMP-2 mRNA was translated into its protein and actively secreted in the medium, as reported in Figure 4.15A. Interestingly, the western blot results obtained detecting MMP2 in the conditioned medium of MUC-1 and TVBF-7 cells demonstrated a significant reduction of MMP2 protein after trabectedin treatment (Figure 4.15B). The secreted MMP2 was functionally active as reported in the zymography assay performed using gels containing gelatin, a MMP2 substrate (Figure 4.15C). Indeed, the signal detected at the expected MMP2 molecular weight was reduced in the conditioned medium obtained from trabectedin-treated cells (trabectedin-treated MUC-1 (mean ± SD) - 45.3% ± 11.5% vs untreated, $p = 0.0012$; trabectedin-treated TVBF-7 cells: -33.8% ± 13.9% vs untreated, $p = 0.0065$). These results strengthen the involvement of MMP2 in the progression and invasiveness in ACC.

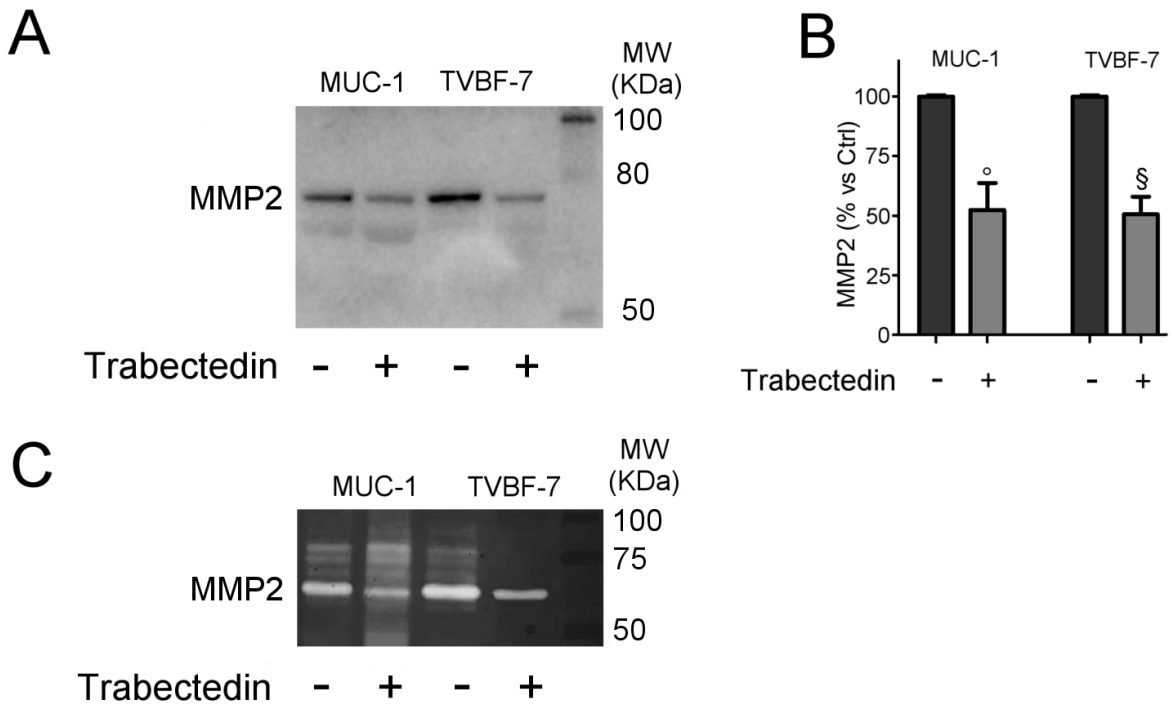

Figure 4.15 Trabectedin effect on MMP2. (A) Representative western blot of MMP2 in the conditioned medium secreted by ACC cells. *(B) Quantification of western blots. Results are presented as % signal of vehicle-treated samples (Ctrl) ± SEM. §P < 0.01; ° P < 0.05. (C) Representative zymogram of MMP2 in the conditioned medium secreted by ACC cells. Each experiment was conducted at least three times.*

5 Discussion

ACC is a rare and aggressive endocrine neoplasm characterized by high morphological, molecular and clinical heterogeneity [99, 100]. Different experimental cell models need to be developed to represent this heterogeneity found in patients, differentiating the models by disease stages, therapeutic responsiveness, genotypes, hormonal phenotypes and gender. For this reason, the development of a new cellular model of ACC with peculiar molecular characteristics represents an important result for both basic and translational research. Until 2016, the only adult human ACC cell line was represented by NCI-H295R cells [89]. These cells, deriving from a primary mitotane-responsive disease, represent only a small subgroup of the ACC. However, patients with advanced metastatic disease and pre-treated disease are those who most urgently require new efficacious pharmacological strategies, especially in case of progression after EDP-M. In recent years, basic and translational research was able to develop several cell lines, resulting from metastatic diseases, among which the first was MUC-1 cells [86]. Further, ACC cell lines of metastatic origin can offer useful models for pharmacological investigation as well as to investigate pathological molecular alteration in these stages, which is specifically challenging in the clinic management and closely related with poor prognosis. Here we reported the development of the new human adult ACC cell line, named TVBF-7. The cell line, derived from the ACC115m primary culture set up in our laboratory, is currently used as a cellular model in several pharmacological studies, two of which were part of my PhD project [103-105, 110]. According to their origin, results indicate, a general lower response to pharmacological treatments for these cells compared to the mitotane-responsive and chemo-naive NCI-H295R cells. An in-depth characterization of TVBF-7 cells was performed in collaboration with Dr. Hantel of the University of Zurich. Evaluation of the mutation status revealed a non-sense APC mutation, never found in the other available adult ACC cell models [88]. The APC gene encodes for the homonymous regulatory protein of the canonical Wnt pathway (Wnt/β-catenin pathway), controlling cytoplasmic β-catenin levels [112]. This pathway is also known to be mutated in NCI-

H295R cells as well, although these cells present a missense mutation in the CTNNB1 gene [113], encoding β-catenin. Based on the known role of Wnt/β-catenin pathway as a driver of ACC [32, 113], new treatments under study at a preclinical level for ACC target this pathway [114]. In this context, the new established TVBF-7 cells could represent a useful model form pharmacological preclinical investigation. Finally, endocrinological characterization revealed high basal cortisol secretion for TVBF-7. These cells are derived from patients without obvious clinical signs of hormonal excess, however, a correlation between APC inactivating mutations and elevated cortisol levels has a been already reported in patients with adrenal tumors [26, 115]. This is an interesting finding, and it underlines the importance to consider the intratumor secretion of cortisol in patients affected by ACC, even if hypercortisolemia is not detected. Indeed, it is well known that the local cortisol secretion in the tumor microenvironment create the immunosuppressive milieu that could account for the resistance to immunotherapy, often observed in ACC patients [62].

From a clinical point of view, ACC pharmacotherapy still lacks effective therapeutic strategies that can be used in the second line. To date, in case of disease progressing after EDP-M, the approach is not standardized [62]. Targeted therapy has led to important changes in the pharmacological management of various malignancies [116]. Molecular investigations described proteins involved in the cell cycle as potential targets in the treatment of ACC [64]. Among them, the CDK4 gene was found overexpressed in more than 60% of ACC samples [65], therefore, cyclin-dependent kinases (CDKs) could be hypothesized as druggable in ACC. To date, three CDK4/6 inhibitors are available for clinical use, namely palbociclib, ribociclib and abemaciclib. Although all of them target CDK4 and CDK6, differences have been reported in terms of pharmacodynamic, pharmacokinetic and toxicological characteristics [101, 117]. We previously demonstrated the effect of palbociclib on NCI-H295R cells and on a set of primary cultures [118]. In this part of the project, we evaluated the effect of ribociclib in different ACC cell models, with a particular focus on a combined setting. Results reported here demonstrated that ribociclib exerted both cytotoxic and

antiproliferative activity in *in vitro* experimental cell models of ACC, with an IC_{50} within the μM concentrations. The evaluation of the mean plasma concentrations and the volume of distribution of ribociclib make the concentrations we used for *in vitro* cell treatments consistent with the dosages usually administered in clinic [119]. In a recent publication, indeed, the glioblastoma tumor tissue concentrations of total ribociclib range from 6.03 to 50.88 μM in patients treated with 600 mg ribociclib QD for 8–14 days, while the plasma concentrations range from 1.26 to 5.44 μM, thus indicating the drug accumulation in lyophilic tissues [120]. Ribociclib interferes with the cell cycle progression, causing its arrest and inducing apoptosis in different cellular models [121, 122]. Our results indicate that ribociclib treatment increased the number of apoptotic cells compared to control cells. Furthermore, we also observe an increase in necrotic cells in NCI-H295R after treatment. Taken together these results suggest that ribociclib caused cell death mainly with an apoptotic mechanism in our cells and underline the relevant effect induced by ribociclib on ACC cells viability and proliferation. Subsequently, to evaluate the effect of ribociclib treatment on the cell cycle progression in ACC cells, we analyzed the cell cycle distribution. We observed an accumulation of cells in G2 phase both in NCI-H295R and MUC-1 cells while an accumulation of cells in G1 phase was reported in TVBF-7 cells. Although ribociclib is a CDK4/6 inhibitor and its role in the G1 phase arrest is well described [123], our observations on the two cell lines are in line with published literature describing a G2 arrest due to ribociclib treatment in germinal cell tumor cell lines, where it is shown that in these cell models, the predicted G1 arrest after ribociclib treatment was bypassed and the cell cycle stopped at the G2 or M phases [124]. The different effects on cell cycle progression in our ACC cells induced by ribociclib exposure could be explain with the possible differences in the molecular setting of each cell models, at the level of protein related to cell cycle progression. The molecular mechanisms underlying this phenomenon will be investigated in future projects. Results of different combined treatment schemes with ribociclib plus progesterone reported a positive interaction between these two drugs, particularly in MUC-1 cells and in TVBF-7 cells. This aspect is even more interesting because MUC-1 cells derived from a heavily treated patient with a metastatic disease, in progression after

EDP-M, as well as the TVBF-7 cells, giving strength to the possible clinical application of this combination. Indeed, the advantage of using progesterone in a combination therapy could be of considerable interest for its possible clinical application, since progesterone and its derivatives are commonly administered in oncological patients, due to their anticachectic effect [125]. The safety of adding megestrol acetate, a progesterone derivative, to the EDP-M scheme in patients with low Performance Status ACC has recently been demonstrated [126]. Furthermore, the association of CDK inhibitors and endocrine therapy is a pharmacological approach already in use in the treatment of breast cancer [127, 128]. It is crucial to point out that both CDK inhibitors and progesterone derivatives have been shown to have manageable safety profiles [125, 129]. Also results about the ternary combination demonstrate a positive relation between ribociclib and the reference drug in ACC, mitotane. For this reason, evidence of a positive relationship between mitotane and a drug such as ribociclib could further strengthen the clinical potential of this combination. Mitotane and ribociclib both interact with CYP3A4, causing opposite effects [130, 131]; furthermore ribociclib is a substrate of this enzyme [119]. The clinical relevance of this interaction is, however, unknown and need to be elucidated. The results on the interaction of ribociclib and/or progesterone and/or mitotane in cellular models of ACC *in vitro* are promising and deserve to be further investigated at a preclinical level by studying the possible intracellular pathways involved in this effect.

DNA alkylation appears to be a critical point for inducing cytotoxicity in ACC, indeed cisplatin is a key component of the EDP-M scheme. Preclinical [62, 109] and clinical [132] evidence supports the role of DNA binders in ACC. Trabectedin is an anti-cancer drug approved for the pharmacological management of soft tissue sarcomas and ovarian cancer [79]. We have previously demonstrated the cytotoxic effect of trabectedin in different experimental cell models of ACC, both of primary and metastatic origin, with a long-lasting effect maintained after the discontinuation of drug treatment [109]. One of the aims of this part of the PhD project was to extend the observation about the cytotoxic and antiproliferative activity also in TVBF-7 cells. Indeed, in this ACC cell model,

trabectedin was shown to be very active, being able to induce cytotoxicity at low nanomolar concentrations. Beside the cytotoxic effect, trabectedin also affected the cell proliferation rate in each ACC experimental cell model, obtained from both primary and metastatic disease, and more importantly, these effects were observed at concentrations reachable in humans at the doses already approved for clinical use [133]. Indeed, an administration of trabectedin at a dose of 1mg/m^2 in 3h induced a mean plasma Cmax of 5.1 ng/mL ± 1.2 [134], while an administration of 1.2 mg/m^2 of trabectedin in 24h revealed a Cmax of 1.4 ng/mL ± 0.65 [135].

Then, these results have been validated in more complex experimental contexts, represented by an *in vivo* model. Thus, we evaluated the antineoplastic effect of trabectedin in zebrafish xenografts of each ACC experimental cell model to assess the efficacy of trabectedin in a more physiological and complex *in vivo* environment. The zebrafish embryos model, although much more simple when compared with mammalian animal models, is now recognized as a good model for the translation process of the data obtained with cell cultures [136-139]. We demonstrated that the amount of drug absorbed by the embryos indicates a concentration consistent with those used in *in vitro* assays, which, as indicated above, are comparable to that found in the plasma of trabectedin-treated patients following administration, according to the dosage schedules for approved indications [133]. Data relating the reduction of the xenograft area confirmed the data obtained with the *in vitro* cell cultures.

In our experimental settings, NCI-H295R cells displayed a lower invasive capability compared to results reported elsewhere [140]. This apparent discrepancy in *in vitro* results could be due to both different cell culture conditions [141] and to technical issues such as, for example, kits from different manufactures.

The cancer cell capability to invade and migrate is a complex process involving a number of different actors in a precise timeline, although the precise timing and intracellular pathways involved in complex and peculiar for each cancer [142]. Accordingly, the metastasizing process in ACC can be due to different molecular mechanisms (for an extensive discussion refer to: [143]). The role of matrix metalloproteinases (MMPs) in the processes of invasion and metastasis of tumor cells is well known

[144]. Volante et al. identified MMP2 as a useful marker for the immunohistochemical diagnosis of ACC. Furthermore, a positive correlation between high MMP2 expression and disease aggressiveness was found [111]. Results reported here support the hypothesis of the involvement of trabectedin on MMP2 secretion and activity in ACC. We cannot exclude, however, that trabectedin may influence the synthesis and secretion of other proteases that may contribute to the inhibition of the invasion process induced by the drug. Indeed, in different cell models, MMP2 and others MMPs have been identified as direct β-catenin transcriptional targets and their expression was found to be regulated by the activating status of Wnt/β-catenin signaling pathway [145].We previously linked the effect of trabectedin in NCI-H295R cells with an inhibitory effect on the Wnt/β-catenin pathway [109]. Furthermore, we demonstrated the cytotoxic activity of trabectedin in both Wnt/β-catenin pathway wild type and mutated ACC cells. The effect of trabectedin on MMP2 observed in the present study, therefore could potentially involve the Wnt/β-catenin pathway, but this hypothesis needs confirmation in a dedicated project.

6 Conclusions

Results presented here highlight the need of different experimental cell models in a rare and heterogenous disease such as ACC. The development in our lab of a new cellular model of human ACC increases the number of the available cell models, each of its own genetic, molecular and drug-sensitivity characteristics.

Furthermore, the results for ribociclib and trabectedin together with those previously published [109, 118] could provide the preclinical rationale for an evaluation of the efficacy of ribociclib and trabectedin in ACC in appropriate clinical trials. Finally, our preclinical investigations on trabectedin paved the way to activate a nominal therapeutic use of lurbinectedin (a trabectedin analogue) in patients with advanced ACC.

7 References

1. O'Hare, A.M.N., Michael J., *The Human Adrenal Cortex: Pathology and Biology – An Integrated Approach*. 1982. Chapter 4: Structure of the adult cortex.
2. De Silva, D.C. and B. Wijesiriwardene, *The adrenal glands and their functions.* Ceylon Med J, 2007. **52**(3): p. 95-100.
3. Burford, N.G., N.A. Webster, and D. Cruz-Topete, *Hypothalamic-Pituitary-Adrenal Axis Modulation of Glucocorticoids in the Cardiovascular System.* Int J Mol Sci, 2017. **18**(10).
4. Kim, A.C., et al., *In search of adrenocortical stem and progenitor cells.* Endocr Rev, 2009. **30**(3): p. 241-63.
5. Lotfi, C.F.P., et al., *The human adrenal cortex: growth control and disorders.* Clinics (Sao Paulo), 2018. **73**(suppl 1): p. e473s.
6. Ishimoto, H. and R.B. Jaffe, *Development and function of the human fetal adrenal cortex: a key component in the feto-placental unit.* Endocr Rev, 2011. **32**(3): p. 317-55.
7. Megha, R.W., C. J. Kashyap, S. Leslie, S. W., *Anatomy, Abdomen and Pelvis, Adrenal Glands (Suprarenal Glands), in StatPearls*. 2022, Treasure Island (FL).
8. Xing, Y., et al., *Development of adrenal cortex zonation.* Endocrinol Metab Clin North Am, 2015. **44**(2): p. 243-74.
9. Kanczkowski, W., M. Sue, and S.R. Bornstein, *The adrenal gland microenvironment in health, disease and during regeneration.* Hormones (Athens), 2017. **16**(3): p. 251-265.
10. Gallo-Payet, N., A. Martinez, and A. Lacroix, *Editorial: ACTH Action in the Adrenal Cortex: From Molecular Biology to Pathophysiology.* Front Endocrinol (Lausanne), 2017. **8**: p. 101.
11. Reimann, M., et al., *Adrenal medullary dysfunction as a feature of obesity.* Int J Obes (Lond), 2017. **41**(5): p. 714-721.
12. Baranowski, E.S., W. Arlt, and J. Idkowiak, *Monogenic Disorders of Adrenal Steroidogenesis.* Horm Res Paediatr, 2018. **89**(5): p. 292-310.
13. Dutt, M.W.C.J.J., I., *Physiology, Adrenal Gland, in StatPearls*. 2022, Treasure Island (FL).
14. Pivonello, C.S., C. Patalano, R. Di Paola, N. Piovanello, R, *Prospettive future nella terapia della Sindrome di Cushing. L'Endocrinologo*, 2022. **23**: p. 606–614.
15. Silverman, M.L. and A.K. Lee, *Anatomy and pathology of the adrenal glands.* Urol Clin North Am, 1989. **16**(3): p. 417-32.
16. Mete, O., et al., *Overview of the 2022 WHO Classification of Adrenal Cortical Tumors.* Endocr Pathol, 2022. **33**(1): p. 155-196.
17. Fassnacht, M., et al., *European Society of Endocrinology Clinical Practice Guidelines on the management of adrenocortical carcinoma in adults, in collaboration with the European Network for the Study of Adrenal Tumors.* Eur J Endocrinol, 2018. **179**(4): p. G1-G46.
18. Fassnacht, M., et al., *Adrenocortical carcinomas and malignant phaeochromocytomas: ESMO-EURACAN Clinical Practice Guidelines for diagnosis, treatment and follow-up.* Ann Oncol, 2020. **31**(11): p. 1476-1490.
19. Ribeiro, R.C. and B. Figueiredo, *Childhood adrenocortical tumours.* Eur J Cancer, 2004. **40**(8): p. 1117-26.
20. Bielinska, M., et al., *Review paper: origin and molecular pathology of adrenocortical neoplasms.* Vet Pathol, 2009. **46**(2): p. 194-210.
21. Herrmann, L.J., et al., *TP53 germline mutations in adult patients with adrenocortical carcinoma.* J Clin Endocrinol Metab, 2012. **97**(3): p. E476-85.
22. Grisanti, S., et al., *Molecular genotyping of adrenocortical carcinoma: a systematic analysis of published literature 2019-2021.* Curr Opin Oncol, 2022. **34**(1): p. 19-28.
23. Karamurzin, Y., et al., *Unusual DNA mismatch repair-deficient tumors in Lynch syndrome: a report of new cases and review of the literature.* Hum Pathol, 2012. **43**(10): p. 1677-87.
24. Li, F.P., et al., *A cancer family syndrome in twenty-four kindreds.* Cancer Res, 1988. **48**(18): p. 5358-62.

25. Gatta-Cherifi, B., et al., *Adrenal involvement in MEN1. Analysis of 715 cases from the Groupe d'etude des Tumeurs Endocrines database.* Eur J Endocrinol, 2012. **166**(2): p. 269-79.
26. Gaujoux, S., et al., *Inactivation of the APC gene is constant in adrenocortical tumors from patients with familial adenomatous polyposis but not frequent in sporadic adrenocortical cancers.* Clin Cancer Res, 2010. **16**(21): p. 5133-41.
27. Weksberg, R., C. Shuman, and A.C. Smith, *Beckwith-Wiedemann syndrome.* Am J Med Genet C Semin Med Genet, 2005. **137C**(1): p. 12-23.
28. Assié, G., et al., *Integrated genomic characterization of adrenocortical carcinoma.* Nat Genet, 2014. **46**(6): p. 607-12.
29. Lerario, A.M., A. Moraitis, and G.D. Hammer, *Genetics and epigenetics of adrenocortical tumors.* Mol Cell Endocrinol, 2014. **386**(1-2): p. 67-84.
30. Zheng, S., et al., *Comprehensive Pan-Genomic Characterization of Adrenocortical Carcinoma.* Cancer Cell, 2016. **29**(5): p. 723-736.
31. Valenta, T., G. Hausmann, and K. Basler, *The many faces and functions of β-catenin.* EMBO J, 2012. **31**(12): p. 2714-36.
32. Gaujoux, S., et al., *β-catenin activation is associated with specific clinical and pathologic characteristics and a poor outcome in adrenocortical carcinoma.* Clin Cancer Res, 2011. **17**(2): p. 328-36.
33. Wasserman, J.D., G.P. Zambetti, and D. Malkin, *Towards an understanding of the role of p53 in adrenocortical carcinogenesis.* Mol Cell Endocrinol, 2012. **351**(1): p. 101-10.
34. Altieri, B., A. Colao, and A. Faggiano, *The role of insulin-like growth factor system in the adrenocortical tumors.* Minerva Endocrinol, 2019. **44**(1): p. 43-57.
35. Gicquel, C., et al., *Rearrangements at the 11p15 locus and overexpression of insulin-like growth factor-II gene in sporadic adrenocortical tumors.* J Clin Endocrinol Metab, 1994. **78**(6): p. 1444-53.
36. Weber, M.M., et al., *Insulin-like growth factor receptors in normal and tumorous adult human adrenocortical glands.* Eur J Endocrinol, 1997. **136**(3): p. 296-303.
37. Giordano, T.J., et al., *Distinct transcriptional profiles of adrenocortical tumors uncovered by DNA microarray analysis.* Am J Pathol, 2003. **162**(2): p. 521-31.
38. Gicquel, C., et al., *Molecular markers and long-term recurrences in a large cohort of patients with sporadic adrenocortical tumors.* Cancer Res, 2001. **61**(18): p. 6762-7.
39. Fassnacht, M., et al., *Management of adrenal incidentalomas: European Society of Endocrinology Clinical Practice Guideline in collaboration with the European Network for the Study of Adrenal Tumors.* Eur J Endocrinol, 2016. **175**(2): p. G1-G34.
40. Cawood, T.J., et al., *Recommended evaluation of adrenal incidentalomas is costly, has high false-positive rates and confers a risk of fatal cancer that is similar to the risk of the adrenal lesion becoming malignant; time for a rethink?* Eur J Endocrinol, 2009. **161**(4): p. 513-27.
41. Berruti, A., et al., *Prognostic role of overt hypercortisolism in completely operated patients with adrenocortical cancer.* Eur Urol, 2014. **65**(4): p. 832-8.
42. Fassnacht, M., et al., *Adrenocortical carcinoma: a clinician's update.* Nat Rev Endocrinol, 2011. **7**(6): p. 323-35.
43. Seccia, T.M., et al., *Aldosterone-producing adrenocortical carcinoma: an unusual cause of Conn's syndrome with an ominous clinical course.* Endocr Relat Cancer, 2005. **12**(1): p. 149-59.
44. Else, T., et al., *Adrenocortical carcinoma.* Endocr Rev, 2014. **35**(2): p. 282-326.
45. Fassnacht, M., et al., *Limited prognostic value of the 2004 International Union Against Cancer staging classification for adrenocortical carcinoma: proposal for a Revised TNM Classification.* Cancer, 2009. **115**(2): p. 243-50.
46. Erdogan, I., et al., *The role of surgery in the management of recurrent adrenocortical carcinoma.* J Clin Endocrinol Metab, 2013. **98**(1): p. 181-91.

47. Beuschlein, F., et al., *Major prognostic role of Ki67 in localized adrenocortical carcinoma after complete resection.* J Clin Endocrinol Metab, 2015. **100**(3): p. 841-9.
48. Elhassan, Y.S., et al., *S-GRAS score for prognostic classification of adrenocortical carcinoma: an international, multicenter ENSAT study.* Eur J Endocrinol, 2021. **186**(1): p. 25-36.
49. Terzolo, M., et al., *Management of adrenal cancer: a 2013 update.* J Endocrinol Invest, 2014. **37**(3): p. 207-17.
50. Sbiera, S., et al., *Mitotane Inhibits Sterol-O-Acyl Transferase 1 Triggering Lipid-Mediated Endoplasmic Reticulum Stress and Apoptosis in Adrenocortical Carcinoma Cells.* Endocrinology, 2015. **156**(11): p. 3895-908.
51. Paragliola, R.M., et al., *Role of Mitotane in Adrenocortical Carcinoma - Review and State of the art.* Eur Endocrinol, 2018. **14**(2): p. 62-66.
52. Robinson, B.G., et al., *The effect of o,p'-DDD on adrenal steroid replacement therapy requirements.* Clin Endocrinol (Oxf), 1987. **27**(4): p. 437-44.
53. Baudin, E., et al., *Impact of monitoring plasma 1,1-dichlorodiphenildichloroethane (o,p'DDD) levels on the treatment of patients with adrenocortical carcinoma.* Cancer, 2001. **92**(6): p. 1385-92.
54. Hermsen, I.G., et al., *Plasma concentrations of o,p'DDD, o,p'DDA, and o,p'DDE as predictors of tumor response to mitotane in adrenocortical carcinoma: results of a retrospective ENS@T multicenter study.* J Clin Endocrinol Metab, 2011. **96**(6): p. 1844-51.
55. Terzolo, M., et al., *Mitotane levels predict the outcome of patients with adrenocortical carcinoma treated adjuvantly following radical resection.* Eur J Endocrinol, 2013. **169**(3): p. 263-70.
56. Fassnacht, M., et al., *Combination chemotherapy in advanced adrenocortical carcinoma.* N Engl J Med, 2012. **366**(23): p. 2189-97.
57. Laganà, M., et al., *Efficacy of the EDP-M Scheme Plus Adjunctive Surgery in the Management of Patients with Advanced Adrenocortical Carcinoma: The Brescia Experience.* Cancers (Basel), 2020. **12**(4).
58. Berruti, A., et al., *Etoposide, doxorubicin and cisplatin plus mitotane in the treatment of advanced adrenocortical carcinoma: a large prospective phase II trial.* Endocr Relat Cancer, 2005. **12**(3): p. 657-66.
59. Grisanti, S., et al., *Clinical Prognostic Factors in Patients With Metastatic Adrenocortical Carcinoma Treated With Second Line Gemcitabine Plus Capecitabine Chemotherapy.* Front Endocrinol (Lausanne), 2021. **12**: p. 624102.
60. Henning, J.E.K., et al., *Gemcitabine-Based Chemotherapy in Adrenocortical Carcinoma: A Multicenter Study of Efficacy and Predictive Factors.* J Clin Endocrinol Metab, 2017. **102**(11): p. 4323-4332.
61. Sperone, P., et al., *Gemcitabine plus metronomic 5-fluorouracil or capecitabine as a second-/third-line chemotherapy in advanced adrenocortical carcinoma: a multicenter phase II study.* Endocr Relat Cancer, 2010. **17**(2): p. 445-53.
62. Cremaschi, V., et al., *Advances in adrenocortical carcinoma pharmacotherapy: what is the current state of the art?* Expert Opin Pharmacother, 2022. **23**(12): p. 1413-1424.
63. Tripathy, D., A. Bardia, and W.R. Sellers, *Ribociclib (LEE011): Mechanism of Action and Clinical Impact of This Selective Cyclin-Dependent Kinase 4/6 Inhibitor in Various Solid Tumors.* Clin Cancer Res, 2017. **23**(13): p. 3251-3262.
64. De Martino, M.C., et al., *Molecular screening for a personalized treatment approach in advanced adrenocortical cancer.* J Clin Endocrinol Metab, 2013. **98**(10): p. 4080-8.
65. Liang, R., et al., *Targeted Gene Expression Profile Reveals CDK4 as Therapeutic Target for Selected Patients With Adrenocortical Carcinoma.* Front Endocrinol (Lausanne), 2020. **11**: p. 219.
66. Chen, P., et al., *Spectrum and Degree of CDK Drug Interactions Predicts Clinical Performance.* Mol Cancer Ther, 2016. **15**(10): p. 2273-2281.

67. Sumi, N.J., et al., *Chemoproteomics Reveals Novel Protein and Lipid Kinase Targets of Clinical CDK4/6 Inhibitors in Lung Cancer.* ACS Chem Biol, 2015. **10**(12): p. 2680-6.
68. Rath, C.M., et al., *Meta-omic characterization of the marine invertebrate microbial consortium that produces the chemotherapeutic natural product ET-743.* ACS Chem Biol, 2011. **6**(11): p. 1244-56.
69. Rinehart, K.L., *Antitumor compounds from tunicates.* Med Res Rev, 2000. **20**(1): p. 1-27.
70. Administration, F.a.D. *Yondelis - Labeling-Package Insert*. 2020 [cited 2023 October 1]; Available from: https://www.accessdata.fda.gov/drugsatfda_docs/label/2018/207953s005lbl.pdf.
71. Agency, E.M. *Yondelis - Product Information*. 2021 [cited 2023 October 1]; Available from: https://www.ema.europa.eu/en/documents/product-information/yondelis-epar-product-information_en.pdf.
72. D'Incalci, M. and C.M. Galmarini, *A review of trabectedin (ET-743): a unique mechanism of action.* Mol Cancer Ther, 2010. **9**(8): p. 2157-63.
73. Zewail-Foote, M. and L.H. Hurley, *Differential rates of reversibility of ecteinascidin 743-DNA covalent adducts from different sequences lead to migration to favored bonding sites.* J Am Chem Soc, 2001. **123**(27): p. 6485-95.
74. Hurley, L.H. and M. Zewail-Foote, *The antitumor agent ecteinascidin 743: characterization of its covalent DNA adducts and chemical stability.* Adv Exp Med Biol, 2001. **500**: p. 289-99.
75. Jin, S., et al., *Ecteinascidin 743, a transcription-targeted chemotherapeutic that inhibits MDR1 activation.* Proc Natl Acad Sci U S A, 2000. **97**(12): p. 6775-9.
76. Scotto, K.W., *ET-743: more than an innovative mechanism of action.* Anticancer Drugs, 2002. **13 Suppl 1**: p. S3-6.
77. Simoens, C., et al., *In vitro interaction between ecteinascidin 743 (ET-743) and radiation, in relation to its cell cycle effects.* Br J Cancer, 2003. **89**(12): p. 2305-11.
78. Pérez-Losada, J., et al., *The chimeric FUS/TLS-CHOP fusion protein specifically induces liposarcomas in transgenic mice.* Oncogene, 2000. **19**(20): p. 2413-22.
79. Larsen, A.K., C.M. Galmarini, and M. D'Incalci, *Unique features of trabectedin mechanism of action.* Cancer Chemother Pharmacol, 2016. **77**(4): p. 663-71.
80. Villalona-Calero, M.A., et al., *A phase I and pharmacokinetic study of ecteinascidin-743 on a daily x 5 schedule in patients with solid malignancies.* Clin Cancer Res, 2002. **8**(1): p. 75-85.
81. Kanzaki, A., et al., *Overcoming multidrug drug resistance in P-glycoprotein/MDR1-overexpressing cell lines by ecteinascidin 743.* Mol Cancer Ther, 2002. **1**(14): p. 1327-34.
82. Creemers, S.G., et al., *MDR1 inhibition increases sensitivity to doxorubicin and etoposide in adrenocortical cancer.* Endocr Relat Cancer, 2019. **26**(3): p. 367-378.
83. Erba, E., et al., *Ecteinascidin-743 (ET-743), a natural marine compound, with a unique mechanism of action.* Eur J Cancer, 2001. **37**(1): p. 97-105.
84. Allavena, P., et al., *Anti-inflammatory properties of the novel antitumor agent yondelis (trabectedin): inhibition of macrophage differentiation and cytokine production.* Cancer Res, 2005. **65**(7): p. 2964-71.
85. Germano, G., et al., *Role of macrophage targeting in the antitumor activity of trabectedin.* Cancer Cell, 2013. **23**(2): p. 249-62.
86. Sigala, S., et al., *An update on adrenocortical cell lines of human origin.* Endocrine, 2022. **77**(3): p. 432-437.
87. Sedlack, A.J.H., et al., *Preclinical Models of Adrenocortical Cancer.* Cancers (Basel), 2023. **15**(11).
88. Sigala, S., et al., *A Comprehensive Investigation of Steroidogenic Signaling in Classical and New Experimental Cell Models of Adrenocortical Carcinoma.* Cells, 2022. **11**(9).
89. Nanba, K., A.R. Blinder, and W.E. Rainey, *Primary Cultures and Cell Lines for In Vitro Modeling of the Human Adrenal Cortex.* Tohoku J Exp Med, 2021. **253**(4): p. 217-232.

90. Hantel, C., et al., *Targeting heterogeneity of adrenocortical carcinoma: Evaluation and extension of preclinical tumor models to improve clinical translation.* Oncotarget, 2016. **7**(48): p. 79292-79304.
91. Chou, T.C. and P. Talalay, *Quantitative analysis of dose-effect relationships: the combined effects of multiple drugs or enzyme inhibitors.* Adv Enzyme Regul, 1984. **22**: p. 27-55.
92. Fragni, M., et al., *Inhibition of Survivin Is Associated with Zoledronic Acid-induced Apoptosis of Prostate Cancer Cells.* Anticancer Res, 2016. **36**(3): p. 913-20.
93. Livak, K.J. and T.D. Schmittgen, *Analysis of relative gene expression data using real-time quantitative PCR and the 2(-Delta Delta C(T)) Method.* Methods, 2001. **25**(4): p. 402-8.
94. Rossini, E., et al., *Cisplatin Cytotoxicity in Human Testicular Germ Cell Tumor Cell Lines Is Enhanced by the CDK4/6 Inhibitor Palbociclib.* Clin Genitourin Cancer, 2021. **19**(4): p. 316-324.
95. Fiorentini, C., et al., *Antisecretive and Antitumor Activity of Abiraterone Acetate in Human Adrenocortical Cancer: A Preclinical Study.* J Clin Endocrinol Metab, 2016. **101**(12): p. 4594-4602.
96. Westerfield, M., *A Guide for the Laboratory Use of Zebrafish (Danio rerio): The Zebrafish Book*. 4th ed ed. 2000, Eugene, OR, USA.
97. Gianoncelli, A., et al., *Adrenocortical Carcinoma Xenograft in Zebrafish Embryos as a Model To Study the In Vivo Cytotoxicity of Abiraterone Acetate.* Endocrinology, 2019. **160**(11): p. 2620-2629.
98. Lee, J.K., et al., *Modulation of trabectedin (ET-743) hepatobiliary disposition by multidrug resistance-associated proteins (Mrps) may prevent hepatotoxicity.* Toxicol Appl Pharmacol, 2008. **228**(1): p. 17-23.
99. Duregon, E., et al., *Dissecting Morphological and Molecular Heterogeneity in Adrenocortical Carcinoma.* Turk Patoloji Derg, 2015. **31 Suppl 1**: p. 98-104.
100. Gara, S.K., et al., *Metastatic adrenocortical carcinoma displays higher mutation rate and tumor heterogeneity than primary tumors.* Nat Commun, 2018. **9**(1): p. 4172.
101. Braal, C.L., et al., *Inhibiting CDK4/6 in Breast Cancer with Palbociclib, Ribociclib, and Abemaciclib: Similarities and Differences.* Drugs, 2021. **81**(3): p. 317-331.
102. Fragni, M., et al., *In vitro antitumor activity of progesterone in human adrenocortical carcinoma.* Endocrine, 2019. **63**(3): p. 592-601.
103. Rossini, E., et al., *Cytotoxic Effect of Progesterone, Tamoxifen and Their Combination in Experimental Cell Models of Human Adrenocortical Cancer.* Front Endocrinol (Lausanne), 2021. **12**: p. 669426.
104. Tamburello, M., et al., *Preclinical Evidence of Progesterone as a New Pharmacological Strategy in Human Adrenocortical Carcinoma Cell Lines.* Int J Mol Sci, 2023. **24**(7).
105. Abate, A., et al., *Ribociclib Cytotoxicity Alone or Combined With Progesterone and/or Mitotane in in Vitro Adrenocortical Carcinoma Cells.* Endocrinology, 2022. **163**(2).
106. Dickson, M.A., *Molecular pathways: CDK4 inhibitors for cancer therapy.* Clin Cancer Res, 2014. **20**(13): p. 3379-83.
107. Lehmann, T.P., T. Wrzesiński, and P.P. Jagodziński, *The effect of mitotane on viability, steroidogenesis and gene expression in NCI-H295R adrenocortical cells.* Mol Med Rep, 2013. **7**(3): p. 893-900.
108. Warde, K.M., et al., *Liver X receptor inhibition potentiates mitotane-induced adrenotoxicity in ACC.* Endocr Relat Cancer, 2020. **27**(6): p. 361-373.
109. Abate, A., et al., *Cytotoxic Effect of Trabectedin In Human Adrenocortical Carcinoma Cell Lines and Primary Cells.* Cancers (Basel), 2020. **12**(4).
110. Abate, A., et al., *Trabectedin impairs invasiveness and metastasis in adrenocortical carcinoma preclinical models.* Endocr Relat Cancer, 2023. **30**(2).

111. Volante, M., et al., *Matrix metalloproteinase type 2 expression in malignant adrenocortical tumors: Diagnostic and prognostic significance in a series of 50 adrenocortical carcinomas.* Mod Pathol, 2006. **19**(12): p. 1563-9.
112. Schneikert, J. and J. Behrens, *The canonical Wnt signalling pathway and its APC partner in colon cancer development.* Gut, 2007. **56**(3): p. 417-25.
113. Tissier, F., et al., *Mutations of beta-catenin in adrenocortical tumors: activation of the Wnt signaling pathway is a frequent event in both benign and malignant adrenocortical tumors.* Cancer Res, 2005. **65**(17): p. 7622-7.
114. Altieri, B., et al., *Next-generation therapies for adrenocortical carcinoma.* Best Pract Res Clin Endocrinol Metab, 2020. **34**(3): p. 101434.
115. Hosogi, H., et al., *Biallelic APC inactivation was responsible for functional adrenocortical adenoma in familial adenomatous polyposis with novel germline mutation of the APC gene: report of a case.* Jpn J Clin Oncol, 2009. **39**(12): p. 837-46.
116. Min, H.Y. and H.Y. Lee, *Molecular targeted therapy for anticancer treatment.* Exp Mol Med, 2022. **54**(10): p. 1670-1694.
117. Tripathy, D., et al., *Ribociclib plus endocrine therapy for premenopausal women with hormone-receptor-positive, advanced breast cancer (MONALEESA-7): a randomised phase 3 trial.* Lancet Oncol, 2018. **19**(7): p. 904-915.
118. Fiorentini, C., et al., *Palbociclib inhibits proliferation of human adrenocortical tumor cells.* Endocrine, 2018. **59**(1): p. 213-217.
119. *Micromedex® (electronic version). Merative, Ann Arbor, Michigan, USA.* . [cited 2021 1 July]; Available from: www.micromedexsolutions.com.
120. Miller, T.W., et al., *Tumor pharmacokinetics and pharmacodynamics of the CDK4/6 inhibitor ribociclib in patients with recurrent glioblastoma.* J Neurooncol, 2019. **144**(3): p. 563-572.
121. Xiong, Y., et al., *Ribociclib, a selective cyclin D kinase 4/6 inhibitor, inhibits proliferation and induces apoptosis of human cervical cancer in vitro and in vivo.* Biomed Pharmacother, 2019. **112**: p. 108602.
122. Li, T., et al., *Ribociclib (LEE011) suppresses cell proliferation and induces apoptosis of MDA-MB-231 by inhibiting CDK4/6-cyclin D-Rb-E2F pathway.* Artif Cells Nanomed Biotechnol, 2019. **47**(1): p. 4001-4011.
123. Ingham, M. and G.K. Schwartz, *Cell-Cycle Therapeutics Come of Age.* J Clin Oncol, 2017. **35**(25): p. 2949-2959.
124. Skowron, M.A., et al., *CDK4/6 inhibition presents as a therapeutic option for paediatric and adult germ cell tumours and induces cell cycle arrest and apoptosis via canonical and non-canonical mechanisms.* Br J Cancer, 2020. **123**(3): p. 378-391.
125. Ruiz Garcia, V., et al., *Megestrol acetate for treatment of anorexia-cachexia syndrome.* Cochrane Database Syst Rev, 2013. **2013**(3): p. CD004310.
126. Turla, A., et al., *Feasibility and Activity of Megestrol Acetate in Addition to Etoposide, Doxorubicin, Cisplatin, and Mitotane as First-Line Therapy in Patients with Metastatic/Unresectable Adrenocortical Carcinoma with Low Performance Status.* Cancers (Basel), 2023. **15**(18).
127. Im, S.A., et al., *Overall Survival with Ribociclib plus Endocrine Therapy in Breast Cancer.* N Engl J Med, 2019. **381**(4): p. 307-316.
128. Boers, J., et al., *Molecular imaging to identify patients with metastatic breast cancer who benefit from endocrine treatment combined with cyclin-dependent kinase inhibition.* Eur J Cancer, 2020. **126**: p. 11-20.
129. Kwapisz, D., *Cyclin-dependent kinase 4/6 inhibitors in breast cancer: palbociclib, ribociclib, and abemaciclib.* Breast Cancer Res Treat, 2017. **166**(1): p. 41-54.
130. Samant, T.S., et al., *Ribociclib Drug-Drug Interactions: Clinical Evaluations and Physiologically-Based Pharmacokinetic Modeling to Guide Drug Labeling.* Clin Pharmacol Ther, 2020. **108**(3): p. 575-585.

131. van Erp, N.P., et al., *Mitotane has a strong and a durable inducing effect on CYP3A4 activity.* Eur J Endocrinol, 2011. **164**(4): p. 621-6.
132. Cosentini, D., et al., *Activity and safety of temozolomide in advanced adrenocortical carcinoma patients.* Eur J Endocrinol, 2019. **181**(6): p. 681-689.
133. *Micromedex® (electronic version). Merative, Ann Arbor, Michigan, USA.* . [cited 2022 June 15]; Available from: https://www.micromedexsolutions.com.
134. van Kesteren, C., et al., *Clinical pharmacology of the novel marine-derived anticancer agent Ecteinascidin 743 administered as a 1- and 3-h infusion in a phase I study.* Anticancer Drugs, 2002. **13**(4): p. 381-93.
135. van Kesteren, C., et al., *Pharmacokinetics and pharmacodynamics of the novel marine-derived anticancer agent ecteinascidin 743 in a phase I dose-finding study.* Clin Cancer Res, 2000. **6**(12): p. 4725-32.
136. Marques, I.J., et al., *Metastatic behaviour of primary human tumours in a zebrafish xenotransplantation model.* BMC Cancer, 2009. **9**: p. 128.
137. Jung, D.W., et al., *A novel zebrafish human tumor xenograft model validated for anti-cancer drug screening.* Mol Biosyst, 2012. **8**(7): p. 1930-9.
138. Tonon, F., et al., *Rapid and cost-effective xenograft hepatocellular carcinoma model in Zebrafish for drug testing.* Int J Pharm, 2016. **515**(1-2): p. 583-591.
139. Bootorabi, F., et al., *Zebrafish as a Model Organism for the Development of Drugs for Skin Cancer.* Int J Mol Sci, 2017. **18**(7).
140. Ferruzzi, P., et al., *Thiazolidinediones inhibit growth and invasiveness of the human adrenocortical cancer cell line H295R.* J Clin Endocrinol Metab, 2005. **90**(3): p. 1332-9.
141. Kurlbaum, M., et al., *Steroidogenesis in the NCI-H295 Cell Line Model is Strongly Affected By Culture Conditions and Substrain.* Exp Clin Endocrinol Diabetes, 2020. **128**(10): p. 672-680.
142. Fares, J., et al., *Molecular principles of metastasis: a hallmark of cancer revisited.* Signal Transduct Target Ther, 2020. **5**(1): p. 28.
143. Lalli, E. and M. Luconi, *The next step: mechanisms driving adrenocortical carcinoma metastasis.* Endocr Relat Cancer, 2018. **25**(2): p. R31-R48.
144. Abdel-Hamid, N.M. and S.A. Abass, *Matrix metalloproteinase contribution in management of cancer proliferation, metastasis and drug targeting.* Mol Biol Rep, 2021. **48**(9): p. 6525-6538.
145. Nguyen, V.H.L., et al., *Wnt/β-catenin signalling in ovarian cancer: Insights into its hyperactivation and function in tumorigenesis.* J Ovarian Res, 2019. **12**(1): p. 122.